



HAL
open science

Spacetime representation of topological phononics

Pierre A. Deymier, Keith Runge, Pierre Lucas, Jerome O. Vasseur

► **To cite this version:**

Pierre A. Deymier, Keith Runge, Pierre Lucas, Jerome O. Vasseur. Spacetime representation of topological phononics. *New Journal of Physics*, 2018, 20 (5), pp.053005. 10.1088/1367-2630/aaba18 . hal-01802050

HAL Id: hal-01802050

<https://hal.science/hal-01802050>

Submitted on 26 Mar 2024

HAL is a multi-disciplinary open access archive for the deposit and dissemination of scientific research documents, whether they are published or not. The documents may come from teaching and research institutions in France or abroad, or from public or private research centers.

L'archive ouverte pluridisciplinaire **HAL**, est destinée au dépôt et à la diffusion de documents scientifiques de niveau recherche, publiés ou non, émanant des établissements d'enseignement et de recherche français ou étrangers, des laboratoires publics ou privés.



Distributed under a Creative Commons Attribution 4.0 International License

PAPER • OPEN ACCESS

Spacetime representation of topological phononics

To cite this article: Pierre A Deymier *et al* 2018 *New J. Phys.* 20 053005

View the [article online](#) for updates and enhancements.

You may also like

- [Self-dual supergravity and twistor theory](#)
Martin Wolf
- [Topological nodal-link phonons, three-fold Dirac and six-fold nodal-point phonons in the insulator SiO₂](#)
Qing-Bo Liu, Zhe-Qi Wang and Hua-Hua Fu
- [Conformal higher spin theory and twistor space actions](#)
Philipp Hähnel and Tristan McLoughlin



PAPER

Spacetime representation of topological phononics

OPEN ACCESS

RECEIVED
29 January 2018ACCEPTED FOR PUBLICATION
27 March 2018PUBLISHED
2 May 2018Pierre A Deymier¹ , Keith Runge¹, Pierre Lucas¹ and Jérôme O Vasseur²¹ Department of Materials Science and Engineering, University of Arizona, Tucson, AZ 85721 United States of America² Institut d'Electronique, de Micro-electronique et de Nanotechnologie, UMR CNRS 8520, Cité Scientifique, F-59652 Villeneuve d'Ascq Cedex, FranceE-mail: deymier@email.arizona.edu**Keywords:** topological phononics, ghost phonons, twistor theory, Dirac phonons, spacetime

Original content from this work may be used under the terms of the [Creative Commons Attribution 3.0 licence](https://creativecommons.org/licenses/by/4.0/).

Any further distribution of this work must maintain attribution to the author(s) and the title of the work, journal citation and DOI.

**Abstract**

Non-conventional topology of elastic waves arises from breaking symmetry of phononic structures either intrinsically through internal resonances or extrinsically via application of external stimuli. We develop a spacetime representation based on twistor theory of an intrinsic topological elastic structure composed of a harmonic chain attached to a rigid substrate. Elastic waves in this structure obey the Klein–Gordon and Dirac equations and possesses spinorial character. We demonstrate the mapping between straight line trajectories of these elastic waves in spacetime and the twistor complex space. The twistor representation of these Dirac phonons is related to their topological and fermion-like properties. The second topological phononic structure is an extrinsic structure composed of a one-dimensional elastic medium subjected to a moving superlattice. We report an analogy between the elastic behavior of this time-dependent superlattice, the scalar quantum field theory and general relativity of two types of exotic particle excitations, namely temporal Dirac phonons and temporal ghost (tachyonic) phonons. These phonons live on separate sides of a two-dimensional frequency space and are delimited by ghost lines reminiscent of the conventional light cone. Both phonon types exhibit spinorial amplitudes that can be measured by mapping the particle behavior to the band structure of elastic waves.

1. Introduction

Our past and current understanding of sound and elastic waves has been nourished essentially by the paradigm of the plane wave and its periodic counterpart (the Bloch wave) in periodic media. This paradigm relies on the four canonical characteristics of waves: frequency (ω); wave vector (k); amplitude (A); and phase (ϕ). Over the past two decades, the fields of phononic crystals and acoustic metamaterials have achieved significant advances in which researchers manipulate the spectral and refractive properties of phonons and sound waves through their host material by exploiting ω and k [1]. The spectral properties of elastic waves include phenomena such as the formation of stop bands in the transmission spectrum due to Bragg-like scattering or resonant processes, as well as the capacity to achieve narrow band spectral filtering by introducing defects in the material's structure. Negative refraction, zero-angle refraction and other unusual refractive properties utilize the complete characteristics of the dispersion relations of the elastic waves, $\omega(k)$, over both frequency and wave number domains.

More recently, renewed attention has been paid to the amplitude and the phase characteristics of the elastic waves. For instance, when sound waves propagate in media under symmetry breaking conditions, they may exhibit amplitudes $A(k) = A_0 e^{i\theta(k)}$ that acquire a geometric phase θ leading to non-conventional topologies [2] and to analogies with the world of quantum mechanics. Here, we take topology to be the description of the shape of the manifold that supports the amplitude solutions for the elastic equations considered. In particular, we will consider non-trivial topologies that arise from broken symmetries. Examples of broken symmetries include time-reversal symmetry, parity symmetry, chiral symmetry and particle–hole symmetry [2]. Symmetry breaking can be achieved in two ways: (a) intrinsic topological phononic structures whereby symmetry breaking occurs

from structural characteristics such as internal resonances, and (b) extrinsic topological phononic structures where external stimuli are applied. For example, elastic waves in an intrinsic topological structure composed of a one-dimensional (1D) harmonic crystal with masses attached to a rigid substrate through harmonic springs have been shown to obey a Dirac-like equation and to possess a spin-like topology [3, 4]. Extrinsic topological phononic structures have been created by applying a periodic spatial modulation of the stiffness of a 1D elastic medium such that its directed temporal evolution breaks time-reversal and parity symmetries [5–11].

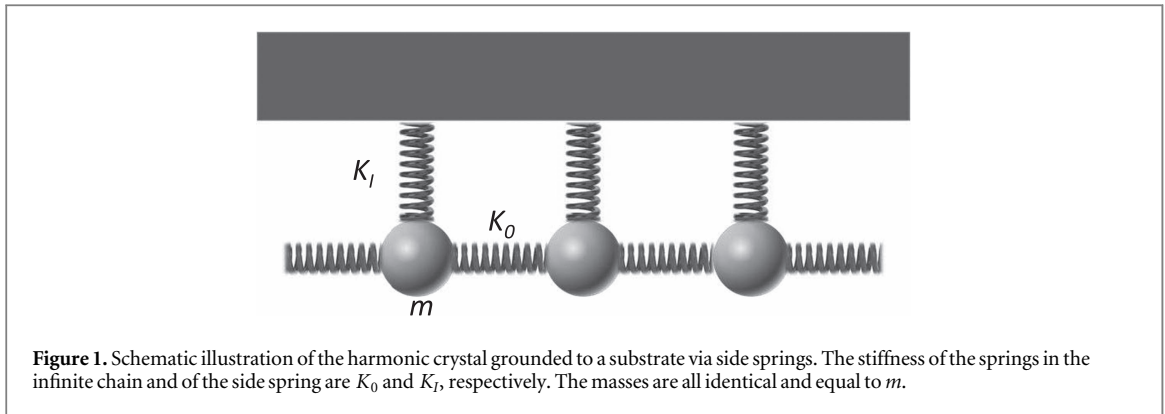
Considerable advances have been made in recent years by the exploration of mechanical analogs of systems that have displayed phase related behavior that leads to topological phononic phenomena. While Dirac factorization is one path that has been taken to obtain these insights, another avenue that has been explored uses the Foucault pendulum as it exemplar [12]. The equations for the topological phononic system are then cast into a form that is analogous to the Schrödinger equation of quantum mechanics. It is noteworthy that the square root of the dynamical matrix which appears in this Schrödinger-like equation also occurs in the Dirac-like equations for topological phononics. Work is ongoing in the development of model systems for the exploration of topological phononics [13] and it is in the spirit of this model development that we proceed with the exploration of other possible exemplars from the physics literature.

The general objective of this work is to establish the foundations for the development of analogies between topological phononics and quantum field theory and geometric spacetime formalisms. This work is motivated by recent and not so recent examples of mechanical dynamical systems analogs of electromagnetic and quantum phenomena. For instance, Maxwell in his seminal paper ‘A dynamical theory of the electromagnetic field’ [14] sought an elastic model of electrical and magnetic phenomena and electromagnetic waves. Mechanical models of quantum phenomena include the localization of ultrasound waves in two-dimensional [15] and three-dimensional [16] disordered media serving as analogs of Anderson localization of electrons. Tunneling of classical waves through phononic crystal barriers established a correspondence with its quantum counterpart [17, 18]. The motion of sound waves in convergent fluid flow exhibits the same properties of motion as electromagnetic waves in gravitational fields in space and time [18]. It has also been shown that dynamical modulation of the dielectric properties of optical materials achieves gauge field analogs. These analogs enable the control of neutral particles like photons [19–23] in ways analogous to charged quantum particles such as electrons. Finally, analogs of superluminal particles such as tachyons, have been reported in unstable mechanical systems [24].

More specifically, in this paper, we develop a spacetime representation of elastic waves supported by the two types of topological phononic structures, namely intrinsic and extrinsic systems. The dynamical equations of motion of the extrinsic structure composed of an infinite linear elastic chain attached to a substrate take on the form of the relativistic Klein–Gordon equation. The Klein–Gordon equation can be Dirac factored revealing that the side springs break time-reversal symmetry and parity symmetry separately. This intrinsic topological elastic structure supports elastic waves which can be characterized by a wave function that possesses both spinorial and orbital components [3, 4]. The elastic wave functions solutions of the Dirac equation effectively represent quasi-standing waves, i.e., a superposition of waves propagating in opposite directions. The spinorial component of the wave function represents the relationship between the amplitude and phase in the space of directions of propagation. In this representation, these Dirac phonons have spin-like properties and fermionic character. In particular, they possess non-conventional topology in wave number space [2]. Here, we analyze the properties of this intrinsic topological elastic structure by representing elastic wave solutions to Klein–Gordon equation and Dirac equations in terms of contour integrals [25]. More specifically, we are able to derive a spin eigenstate equation for Dirac phonons in the intrinsic structure. Dirac phonons are shown to possess half-integer spin eigen values. Furthermore, the contour integral approach enables us to develop a twistor theory [26] of elastic waves. We demonstrate the mapping between straight line trajectories of elastic waves in spacetime and the twistor complex space.

We note, as an aside, that the development of a twistor theory of elastic waves uses the invocation of the Riemann sphere which has been used for other purposes in the analysis of topological materials. Most significantly, the implementation of a Riemann sphere analysis has been used for the determination of Chern invariants in the context of photonic media [27]. The technique has also been applied to topological indices for continuous photonic materials [28]. In the current context, the Riemann sphere is invoked as an instrument toward the construction of an elastic wave twistor representation.

The twistor representation of elastic waves is then used to characterize their phase properties relative to the wave number and tie into the notion of Berry phase [29]. The second topological phononic structure is an extrinsic structure composed of a 1D elastic media subjected to a moving superlattice. These modulations are known to break parity and time-reversal symmetry leading to bulk phonon modes with non-conventional topology [2]. The band structure of a spatio-temporally modulated 1D medium exhibits spectral non-reciprocity e.g., possesses band gaps that form on one side of the first Brillouin zone and not the other. Here, we demonstrate an analogy between the 1D phonons in the vicinity of symmetry breaking conditions (band gap



asymmetry in momentum space) and two types of particle excitations. These particles are not defined in the conventional $(1 + 1)$ spacetime but in a one space and two times domains $(1 + 2)$. For that reason, we call these excitations temporal Dirac phonons and temporal ghost phonons. The wave function of these phonons has spinorial character associated with fermionic behavior. The Dirac phonons possess the analog of a real ‘mass’ but, in contrast, the ghost phonons possess the equivalent of an imaginary mass. The temporal Dirac phonons and ghost phonons exist on two sides of a limiting line in 2D time which is analogous to the speed of light in conventional 2D spacetime. The behavior of temporal ghost phonons is analogous to that of tachyons [30]. There is a one-to-one correspondence between the dispersion relation of elastic waves in the time-dependent superlattice and the spinorial components of the temporal Dirac and ghost phonons, thus enabling measurement of the properties of these temporal particles. Finally, we illustrate additional properties of temporal Dirac phonons and temporal ghost phonons through geometric representations on manifolds in 2D time. We finally address the geometrical description of the dynamics of Dirac and ghost phonons in the form of a geodesic in a complex curved 2D spacetime.

In section 2, we develop the spacetime representation in the context of twistor theory for the intrinsic topological phononic structure. Section 3 focuses on the extrinsic topological phononic structure and its representation in terms of quantum field theory and general relativity. Finally, in section 4, we draw conclusions on the spacetime representation of topological elastic waves in terms of Dirac phonons, twistors, temporal Dirac phonons and temporal ghost phonons. In particular, we address the possibility of analogies between topological phononics, quantum field theory and spacetime representations, which open new avenues for the investigation of exquisite phenomena that previously have only been theorized.

2. Spacetime representation of intrinsic topological acoustic structure

2.1. Topological fermion-like elastic waves

To put our current advances in context and for clarity, we recall some previously derived equations, particularly equations of the same form as the Klein–Gordon and Dirac equations, for the elastic structure composed of a 1D harmonic crystal grounded to a rigid substrate (see figure 1). Solutions to these equations will be analyzed in the twistor representation.

The dynamical equation takes the form of the discrete Klein–Gordon equation:

$$m \frac{\partial^2 u_i}{\partial t^2} - K_0(u_{i+1} - 2u_i + u_{i-1}) + K_I u_i = 0. \quad (1)$$

Equation (1) involves the second derivatives with respect to continuous time and the discrete second derivative of the displacement u_i with respect to position along the crystal, i . In the long wavelength limit equation (1) can be rewritten in the form of the Klein–Gordon equation:

$$\frac{\partial^2 u}{\partial t^2} - \beta^2 \frac{\partial^2 u}{\partial x^2} + \alpha^2 u = 0 \quad (2)$$

with $\alpha^2 = K_I/m$ and $\beta^2 = K_0/m$. We note, in passing, that the Klein–Gordon equation is time-reversal invariant as the second time derivative appears in the equation, such that $t \rightarrow -t$ does not affect the form of the equation.

If we define $X = x/\beta$, equation (2) takes on the simpler form:

$$\frac{\partial^2 u}{\partial t^2} - \frac{\partial^2 u}{\partial X^2} + \alpha^2 u = 0. \quad (3)$$

Making the change of variables:

$$\begin{cases} \lambda = \pm i\alpha(t - X) \\ \mu = \pm i\alpha(t + X) \end{cases} \quad (4)$$

it is straightforward to show that equation (3) reduces to:

$$\frac{\partial^2 u}{\partial \lambda \partial \mu} = u. \quad (5)$$

There exist an infinite number of solutions to equation (5) which take the general form of contour integral in the complex plane [31]:

$$\varphi_n(\lambda, \mu) = \frac{1}{2\pi i} \oint e^{\frac{1}{2}(\lambda z + \mu \frac{1}{z})} \frac{1}{z^{n+1}} dz. \quad (6)$$

The functions given by equation (6) have the following property:

$$\begin{cases} \frac{\partial}{\partial \lambda} \varphi_n = \varphi_{n-1} \\ \frac{\partial}{\partial \mu} \varphi_{n-1} = \varphi_n. \end{cases} \quad (7)$$

Equation (7) represents the Dirac factorization of the Klein–Gordon equation. Indeed, substituting the variables t and X using equation (4) into (7) leads to the Dirac-like equation [32]:

$$\left[\sigma_x \frac{\partial}{\partial t} + i\beta \sigma_y \frac{\partial}{\partial X} \mp i\alpha I \right] \Psi = 0, \quad (8)$$

where σ_x and σ_y are the 2×2 Pauli matrices: $\begin{pmatrix} 0 & 1 \\ 1 & 0 \end{pmatrix}$ and $\begin{pmatrix} 0 & -i \\ i & 0 \end{pmatrix}$ and I is the 2×2 identity matrix.

Note that taking $t \rightarrow -t$ now does not recover the form of equation (8) nor does taking $x \rightarrow -x$, however taking both $t \rightarrow -t$ and $x \rightarrow -x$ recovers the two Dirac-like equations in equation (8). Hence, the Dirac-like equations break time-reversal (T) symmetry and parity (P) symmetry individually but do not break the product PT symmetry. Symmetry breaking arises from the distinction between forward and backward propagating modes and occurs for non-zero values of α .

The solutions of equation (8) are 2×1 spinors:

$$\Psi = \begin{pmatrix} \varphi_n \\ \varphi_{n-1} \end{pmatrix}. \quad (9)$$

The \mp corresponding to the two Dirac-like equation (8) arises from the \pm in equation (4).

We now write the solutions in Fourier form:

$$\Psi_k = \Psi(k, \omega_k) = \xi_k(k, \omega_k) e^{i\omega_k t} e^{ikX}, \quad (10)$$

where

$$\xi_k = \begin{pmatrix} a_n \\ a_{n-1} \end{pmatrix}. \quad (11)$$

Inserting equations (10) and (11) into (8) (choosing the ‘ $-$ ’ sign for illustrative purpose) gives the recursive expressions:

$$\begin{cases} (\omega - k)a_n = \alpha a_{n-1} \\ (\omega + k)a_{n-1} = \alpha a_n. \end{cases} \quad (12)$$

The set of linear equation (12) has non-trivial solutions if the determinant of the matrix $\begin{pmatrix} \omega - k & -\alpha \\ -\alpha & \omega + k \end{pmatrix}$ vanishes, this conditions leads to the dispersion relation:

$$\omega = \pm \sqrt{\alpha^2 + k^2}. \quad (13)$$

The elastic band structure of the harmonic chain attached to a rigid substrate exhibits a gap in its frequency spectrum at $k = 0$. This gap was shown to result from hybridization (or resonance) between the two $\alpha = 0$ dispersion curves, $\omega = k$ and $\omega = -k$, upon attachment of the harmonic chains to the substrate via side springs with non-zero α . For the sake of simplicity, we will limit ourselves from now on to positive ω .

Let us start the recursion relations (12) at $n = 1$, we then have:

$$\begin{pmatrix} a_1 \\ a_0 \end{pmatrix} = a \begin{pmatrix} \sqrt{\omega + k} \\ \sqrt{\omega - k} \end{pmatrix}, \tag{14}$$

where a is some constant. The breaking of T or P symmetry in the Dirac equation leads to a projection of the solutions onto the space of directions of propagation. The spinorial solutions have forward and backward propagating elastic waves which amplitudes are not independent of each other and are related according to equation (14) for example.

For $n = 2$ and using $a_1 = a\sqrt{\omega + k}$, equation (12) reduces to a single equation which solution is $a_2 = a\frac{\omega+k}{\sqrt{\omega-k}}$. Inserting this solution into equation (12) for $n = 3$, yields $a_3 = a\frac{(\omega+k)^{3/2}}{\omega-k}$, etc. The general solution takes the form:

$$a_n = a\frac{(\omega + k)^{n/2}}{(\omega - k)^{(n-1)/2}}. \tag{15}$$

The recurring solutions are therefore:

$$a_{n+1} = \frac{\sqrt{\omega + k}}{\sqrt{\omega - k}} a_n. \tag{16}$$

Let us now consider some additional properties of the solutions $\varphi_n(\lambda, \mu)$ (equation (6)). By making the change of variable $z = \frac{y}{\lambda}$, equation (6) can be rewritten as [31]:

$$\varphi_n(\lambda, \mu) = \lambda^n \frac{1}{2\pi i} \oint e^{\frac{1}{2}(y+\lambda\mu\frac{1}{y})} \frac{1}{y^{n+1}} dy = \lambda^n f_n(\lambda\mu). \tag{17}$$

In equation (17) f_n is a function of the product $\lambda\mu$.

This form reveals that φ_n must satisfy the spin eigenstates equation:

$$\left(\lambda \frac{\partial}{\partial \lambda} - \mu \frac{\partial}{\partial \mu} \right) \varphi_n = n \varphi_n. \tag{18}$$

Converting equation (18) back into conventional spacetime (X, t) and taking its two-dimensional Fourier transform results in:

$$\left(k \frac{\partial}{\partial \omega} - \omega \frac{\partial}{\partial k} \right) \tilde{\varphi}_n = \frac{n}{2} \tilde{\varphi}_n, \tag{19}$$

where $\tilde{\varphi}_n = \tilde{\varphi}_n(\omega, k)$ is the spatio-temporal Fourier transform of $\varphi_n(X, t)$. The solutions of the Klein–Gordon equation, which are labeled by the index n , can therefore take on spin eigen values of $0, \frac{1}{2}, 1, \frac{3}{2}, \dots$

However, if we apply the operator $\left(k \frac{\partial}{\partial \omega} - \omega \frac{\partial}{\partial k} \right)$ on the solutions of the Dirac equations, a_n , one finds that:

$$\left(k \frac{\partial}{\partial \omega} - \omega \frac{\partial}{\partial k} \right) a_n = \left(n - \frac{1}{2} \right) a_n. \tag{20}$$

The solutions of the Dirac equations are a subset of the solutions of the Klein–Gordon equation which have spin eigen values that are multiples of $\frac{1}{2}$. To shed light on the meaning of a $3/2$ spin in the context of elastic waves, we write the three Dirac-like equations for $n = 0, 1, 2$ in spacetime, that is:

$$\begin{cases} \frac{\partial \varphi_0}{\partial t} - \frac{\partial \varphi_0}{\partial X} = i\alpha \varphi_{-1} \\ \frac{\partial \varphi_{-1}}{\partial t} + \frac{\partial \varphi_{-1}}{\partial X} = i\alpha \varphi_0 \\ \frac{\partial \varphi_1}{\partial t} - \frac{\partial \varphi_1}{\partial X} = i\alpha \varphi_0 \\ \frac{\partial \varphi_0}{\partial t} + \frac{\partial \varphi_0}{\partial X} = i\alpha \varphi_1 \\ \frac{\partial \varphi_2}{\partial t} - \frac{\partial \varphi_2}{\partial X} = i\alpha \varphi_1 \\ \frac{\partial \varphi_1}{\partial t} + \frac{\partial \varphi_1}{\partial X} = i\alpha \varphi_2. \end{cases}$$

We can recombine these equations in the form:

$$\frac{\partial \varphi_0}{\partial t} - \frac{\partial \varphi_0}{\partial X} = i\alpha \varphi_{-1} \quad (21a)$$

$$\frac{\partial \varphi_{-1}}{\partial t} + \frac{\partial \varphi_{-1}}{\partial X} = \frac{\partial \varphi_1}{\partial t} - \frac{\partial \varphi_1}{\partial X} \quad (21b)$$

$$\frac{\partial \varphi_0}{\partial t} + \frac{\partial \varphi_0}{\partial X} = \frac{\partial \varphi_2}{\partial t} - \frac{\partial \varphi_2}{\partial X} \quad (21c)$$

$$\frac{\partial \varphi_1}{\partial t} + \frac{\partial \varphi_1}{\partial X} = i\alpha \varphi_2. \quad (21d)$$

The spinor $\begin{pmatrix} \varphi_{-1} \\ \varphi_2 \end{pmatrix}$ which has spin eigen values of $-3/2$ and $+3/2$ can be visualized as the superposition of spin 1 (-1) objects combined with spin $1/2$ ($-1/2$) objects. Considering plane wave solutions in equation (21b), the backward propagating φ_{-1} is identical to the forward propagating, φ_1 . Equation (21c) states that the forward φ_2 is identical to the backward propagating, φ_0 . However, these two equations do not impose any relationship (constraint) on the possible directions of propagation of φ_0 and φ_1 . Equations (21a) and (21d) in contrast set constraints on φ_{-1} being equivalent to a forward propagating φ_0 and φ_2 being a backward propagating φ_1 . The amplitudes of the spinor $\begin{pmatrix} \varphi_{-1} \\ \varphi_2 \end{pmatrix}$ are therefore not independent of each other. They possess fermionic character (spin eigen value $\pm 1/2$) [2]. It represents an elastic wave which is the superposition of a forward and a backward propagating wave with amplitude related to each other. The quantities φ_0 and φ_1 do not form a spinor as their amplitudes in the forward or backward directions of propagation are independent of each other. They possess bosonic character and therefore spin eigen values ± 1 . This argument can be extended to other solutions with spin eigen values of $5/2, 7/2$, etc with increasing number of boson-like elastic waves and still two fermion-like waves.

2.2. Twistor space representation of topological elastic waves

In this section, we explore the spatio-temporal properties of the solutions of Klein–Gordon equation (as well as Dirac equations) given by equation (6). We rewrite equation (6) in terms of time, t , space X , and a new space-like variable ζ :

$$\phi_n(t, X, \zeta) = \frac{1}{2\pi i} 2 \oint e^{\frac{1}{2}i\alpha \left[\left(z + \frac{1}{z}\right)t - \left(z - \frac{1}{z}\right)X \pm 2\zeta \right]} \frac{1}{z^{n+1}} dz. \quad (22)$$

In this form, ϕ_n is solution of the equation:

$$\frac{\partial^2 \phi_n}{\partial t^2} - \frac{\partial^2 \phi_n}{\partial X^2} - \frac{\partial^2 \phi_n}{\partial \zeta^2} = 0. \quad (23)$$

Because of the second derivative with respect to ζ in equation (23), the sign in front of the 2ζ in equation (22) is arbitrary. We will use $+$ in the rest of the section. In equation (23) ζ plays the role of a second spatial variable. Equation (23) is the usual elastic equation for a two-dimensional medium. It represents a model of the harmonic chain attached to a substrate in a $(2 + 1)$ spacetime.

The argument of the exponential in equation (22) can be rewritten in the form of a second-order polynomial in z :

$$i\alpha \frac{1}{z} \left[\frac{1}{2}(X + t) + \zeta z - \frac{1}{2}(X - t)z^2 \right] = i\alpha \frac{1}{z} \eta. \quad (24)$$

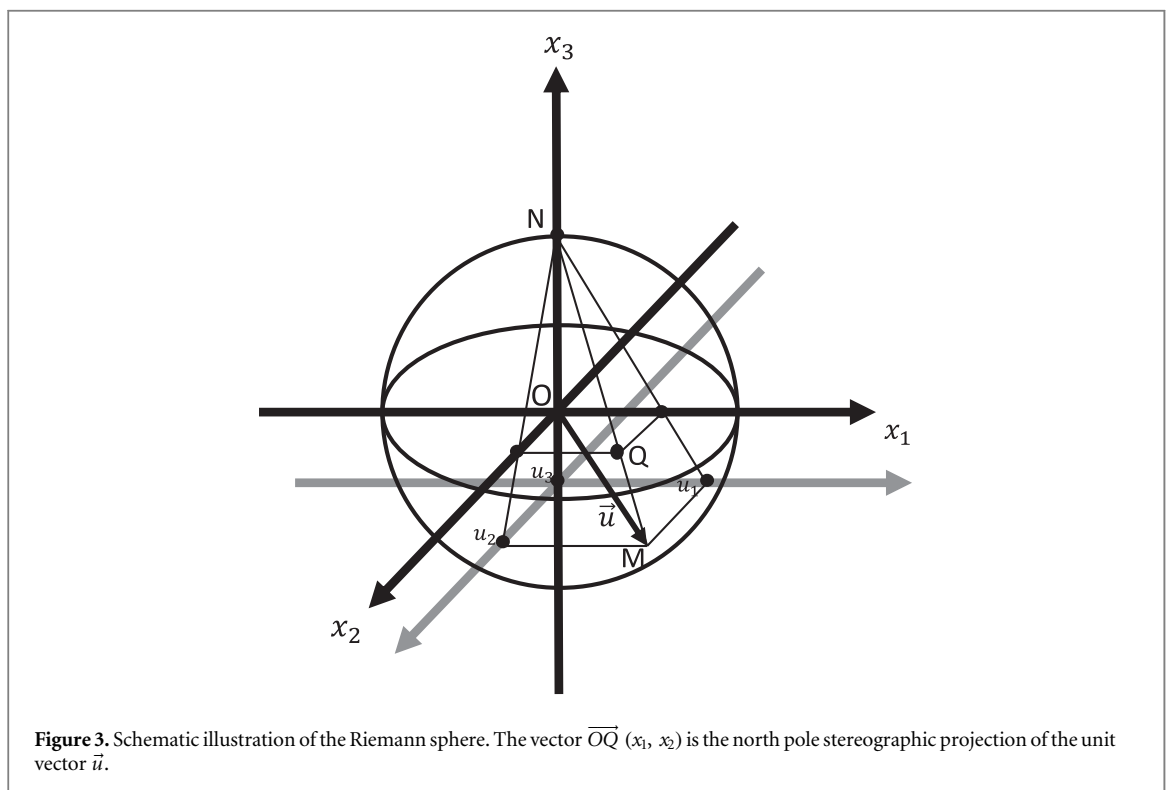
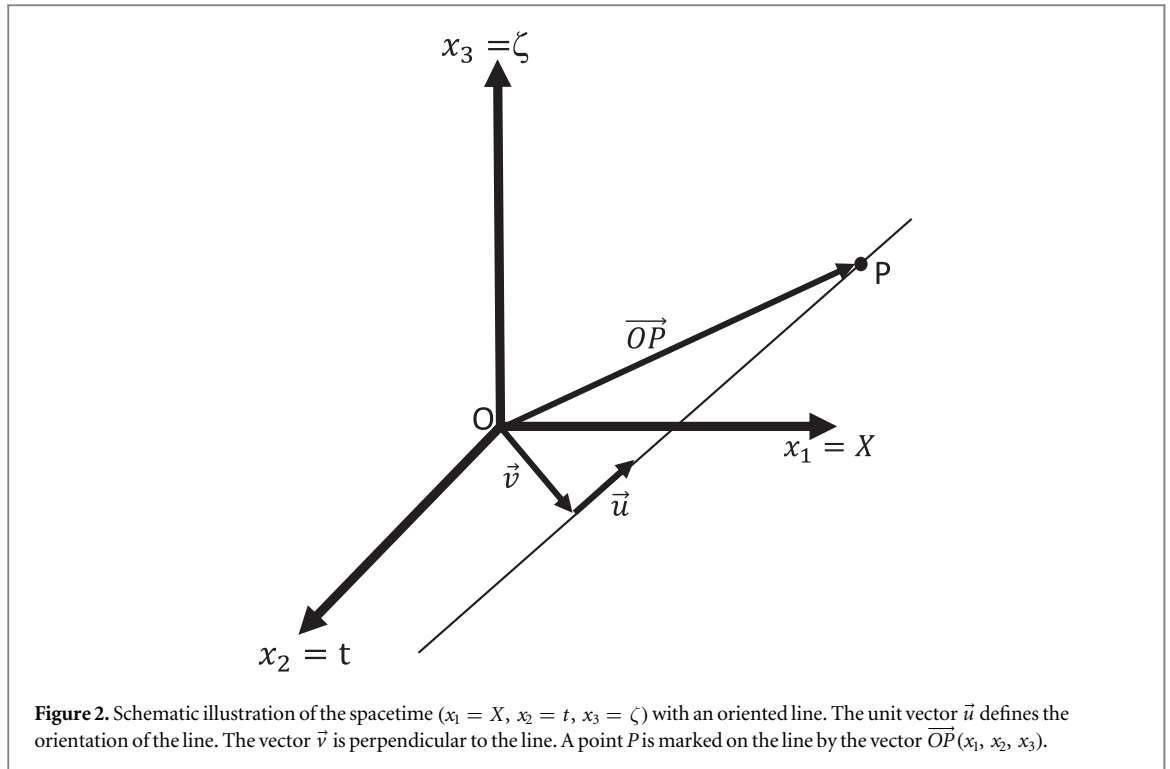
The square bracket η takes the form of an incidence relation between spacetime ($x_1 = X$, $x_2 = t$, $x_3 = \zeta$) and twistor space [26]. Let us consider a directed line in (x_1, x_2, x_3) as shown in figure 2.

The vector \overrightarrow{OP} is given by:

$$\overrightarrow{OP} = \vec{v} + L\vec{u}, \quad (25)$$

where L is a length along the line from the end of vector \vec{v} to the point P . We also have the relations $\vec{u} \cdot \vec{v} = 0$ and $\vec{u} \cdot \vec{u} = 1$. All the orientation vectors \vec{u} can be illustrated on the unit sphere or Riemann sphere. We can now consider the stereographic projection of the orientation unit vector \vec{u} from the north pole of the Riemann sphere (see figure 3).

The coordinates of the projection vector \overrightarrow{OQ} are $x_1 = \frac{u_1}{1 - u_3}$ and $x_2 = \frac{u_2}{1 - u_3}$. If we complexify the plane (x_1, x_2) by identifying the axis x_2 with the imaginary axis the stereographic projection of the unit vector \vec{u} can be defined as:



$$\sigma(\vec{u}) = \frac{u_1 + iu_2}{1 - u_3}. \tag{26}$$

We now introduce a parametric equation for the unit vector $\vec{u}(s)$. The parameters defines a path followed by the end of the vector \vec{u} on the Riemann sphere. The directional derivative of $\sigma(\vec{u})$ takes the form:

$$\eta = \frac{\partial \sigma}{\partial s} = \frac{\partial \sigma}{\partial \vec{u}} \frac{\partial \vec{u}}{\partial s} = \frac{\partial \sigma}{\partial \vec{u}} \vec{v}. \tag{27}$$

In equation (27) $\frac{\partial \vec{u}}{\partial s} = \vec{v}$ is a tangent vector to the parameterized path on the Riemann sphere. Using equations (25)–(27), we find the condition that gives the set of oriented lines going through a point P . After a lengthy set of algebraic manipulations, one finds:

$$\eta = \frac{1}{2}(x_1 + ix_2) + \sigma x_3 - \frac{1}{2}(x_1 - ix_2)\sigma^2. \tag{28}$$

Equation (28) is equivalent to the square bracket terms in equation (24). This incidence relation maps the spacetime $(x_1 = X, x_2 = t, x_3 = \zeta)$ to the twistor space defined by the pair of complex numbers, (σ, η) . A line in spacetime (i.e., a linear trajectory) maps into a point in twistor space. The set of all lines which go through a point P in spacetime becomes the Riemann sphere in twistor space.

2.3. Twistor space and topological phonics

2.3.1. Fourier representation of the incidence relation

By inserting equation (24) into (22), we can rewrite the solution of the elastic problem as:

$$\phi_n(t, X, \zeta) = \frac{1}{2\pi i} 2 \oint e^{i\alpha \frac{1}{z} \left[\frac{1}{2}(X+t) + \zeta z - \frac{1}{2}(X-t)z^2 \right]} \frac{1}{z^{n+1}} dz \tag{29}$$

or

$$\phi_n(t, X, \zeta) = \frac{1}{2\pi i} \oint f_n \left(z, \eta = \frac{1}{2}(X + t) + \zeta z - \frac{1}{2}(X - t)z^2 \right) dz. \tag{30}$$

We can rewrite

$$\eta = (1 + z^2) \left[t + \frac{1 - z^2}{1 + z^2} X + \frac{2z}{1 + z^2} \zeta \right] \tag{31}$$

and redefine the complex z in terms of complex quantities on the unit circle

$$\begin{cases} \frac{1 - z^2}{1 + z^2} = \cos \theta = \frac{e^{i\theta} + e^{-i\theta}}{2} \\ \frac{2z}{1 + z^2} = \sin \theta = \frac{e^{i\theta} - e^{-i\theta}}{2i}. \end{cases} \tag{32}$$

Equation (30) can be re-expressed in terms of the complex quantities $\gamma = e^{i\theta}$, $q = X + i\zeta$ and their complex conjugates $\bar{\gamma} = e^{-i\theta}$ and $\bar{q} = X - i\zeta$:

$$\phi_n(t, X, \zeta) = \frac{1}{2\pi i} \oint f_n \left(\gamma, t + \frac{1}{2}\bar{q}\gamma + \frac{1}{2}q\bar{\gamma} \right) d\gamma. \tag{33}$$

We now make the connection with Fourier representation of elastic waves, that is, plane waves in our elastic system. We rewrite the complex, γ in the form:

$$\gamma = e^{i\theta} = \frac{k}{\sqrt{k^2 + \alpha^2}} + i \frac{\alpha}{\sqrt{k^2 + \alpha^2}}, \tag{34}$$

where k is a wave number along the harmonic chain. The incidence relation in equation (33) then becomes:

$$t + \frac{1}{2}\bar{q}\gamma + \frac{1}{2}q\bar{\gamma} = \frac{1}{\sqrt{k^2 + \alpha^2}} (\sqrt{k^2 + \alpha^2} t + kX + \alpha\zeta). \tag{35}$$

Since the dispersion relation for the harmonic chain attached to a rigid substrate is $\omega = \sqrt{k^2 + \alpha^2}$, the term in parenthesis of equation (35) becomes the usual exponent of a plane wave $(\omega t + kX + \alpha\zeta)$ obeying equation (23).

2.3.2. Spinor representation of the incidence relation

Equation (22) states that solutions to the elastic Klein–Gordon equation (and, by the same token, some of the solutions to the elastic Dirac equation), can be formulated as:

$$\phi_n(\lambda, \mu, \zeta) = \frac{1}{2\pi i} \oint f_n \left(z, \frac{1}{2}\lambda z + \frac{1}{2}\mu \frac{1}{z} + i\alpha\zeta \right) dz. \tag{36a}$$

Since the incidence relation appears in an exponent in equation (22), we can reformulate equation (22) in terms of a product of exponential functions. Equation (36a) can then be rewritten in the form:

$$\phi_n(\lambda, \mu, \zeta) = \frac{1}{2\pi i} \oint f_n(z, \lambda z + i\alpha\zeta, \mu + i\alpha\zeta) dz. \quad (36b)$$

In equation (36b), we have redefined the incidence relations in terms of two quantities, $\Pi_1 = \frac{1}{i\alpha}\lambda z + \zeta$ and $\Pi_2 = \frac{1}{i\alpha}\mu + \zeta z$, which form a spinor $\Pi = \begin{pmatrix} \Pi_1 \\ \Pi_2 \end{pmatrix}$. This spinor is effectively the product of a 2×2 matrix with

another spinor $\Sigma = \begin{pmatrix} \Sigma_1 \\ \Sigma_2 \end{pmatrix} = \begin{pmatrix} 1 \\ z \end{pmatrix}$. The incidence relation becomes:

$$\Pi = \begin{pmatrix} \Pi_1 \\ \Pi_2 \end{pmatrix} = \begin{pmatrix} \zeta & \lambda/i\alpha \\ \mu/i\alpha & \zeta \end{pmatrix} \begin{pmatrix} \Sigma_1 \\ \Sigma_2 \end{pmatrix} = \begin{pmatrix} \zeta & t - X \\ t + X & \zeta \end{pmatrix} \begin{pmatrix} \Sigma_1 \\ \Sigma_2 \end{pmatrix} = \mathbf{R}\Sigma, \quad (37)$$

where, \mathbf{R} , is the incidence matrix. If the oriented propagation of an acoustic wave, represented by $\{\Pi, \Sigma\}$ in twistor space, passes through the point (t, X, ζ) in spacetime, then the incidence relation (37) is satisfied.

The incidence matrix can be reformulated in Fourier space as a differential operator, namely:

$$\tilde{\mathbf{R}} = \begin{pmatrix} \frac{\partial}{\partial\alpha} & \frac{\partial}{\partial\omega} - \frac{\partial}{\partial k} \\ \frac{\partial}{\partial\omega} + \frac{\partial}{\partial k} & \frac{\partial}{\partial\alpha} \end{pmatrix}. \quad (38)$$

In the previous section, we have shown that in Fourier space, the complex z , can be replaced by the quantity $\gamma = \frac{k+i\alpha}{\sqrt{k^2+\alpha^2}}$, that is we can write $\tilde{\Sigma} = \begin{pmatrix} 1 \\ \gamma \end{pmatrix}$. We note that because α represents effectively the stiffness of the side springs of the elastic system, it is a constant. The complex quantity γ spans half of the equator of the Riemann sphere from -1 to $+1$ when $k \in [-\infty, +\infty]$. For $k = 0$, $\gamma = i$. Using equation (37), we obtain:

$$\tilde{\Pi} = \begin{pmatrix} -\frac{\partial\gamma}{\partial k} \\ 0 \end{pmatrix} = \begin{pmatrix} -i\frac{\alpha}{k^2+\alpha^2} \\ 0 \end{pmatrix}. \quad (39)$$

After calculating the product, $\tilde{\Pi}\tilde{\Sigma} = i\frac{\alpha}{k^2+\alpha^2}$, which is isomorphic to the Berry connection [29], we can obtain the phase accumulated by elastic waves as $k \in [-\infty, +\infty]$ using the equation:

$$\delta = i \int_{-\infty}^{+\infty} \tilde{\Pi}\tilde{\Sigma} dk = \int_{-\infty}^{+\infty} \frac{\alpha}{k^2+\alpha^2} dk = \pi. \quad (40)$$

The elastic waves solutions of the Klein–Gordon equation accumulate a phase of π as one moves along the dispersion curve of the harmonic chain attached to a rigid substrate. Each direction of propagation $k < 0$ and $k > 0$ contribute $\frac{\pi}{2}$ to the total phase [2].

3. Spacetime representation of an extrinsic topological phononic structure

3.1. Time-dependent superlattice

In considering the systems with spatio-temporal modulations, we note that the topic of spatial and temporal modulation has seen a great deal of interest and activity in the context of electromagnetic interactions with modulated material [33–35]. Here we will turn our interest to elastic systems with spatio-temporal modulations.

The model system of an extrinsic topological acoustic system is a 1D elastic system subjected to a spatio-temporal modulation of its stiffness. This system was described elsewhere [5] and here we review some of its main features that will lead to this paper's general relativistic description of its properties. In [5], we noted that, for this system, the bulk elastic wave functions are supported in the momentum space manifold by a non-conventional torsional topology of a Möbius strip with a single twist. In the long wavelength limit, propagation of longitudinal elastic waves in a 1D medium perturbed by a spatio-temporal modulation of its stiffness, $C(x, t)$, obeys the following equation of motion:

$$\rho \frac{\partial^2 u(x, t)}{\partial t^2} = \frac{\partial}{\partial x} \left(C(x, t) \frac{\partial u(x, t)}{\partial x} \right) = C(x, t) \frac{\partial^2 u(x, t)}{\partial x^2} + \frac{\partial C(x, t)}{\partial x} \frac{\partial u(x, t)}{\partial x}. \quad (41)$$

In equation (41), $u(x, t)$ is the displacement field and ρ is the mass density of the medium. As opposed to the system of figure 1, the side springs K_I are not present and the stiffness of the continuous system is modulated in time and space. We consider a sinusoidal variation of the stiffness with position and time:

$$C(x, t) = C_0 + 2C_1 \sin(Kx + \Omega t), \quad (42)$$

where C_0 and C_1 are positive constants. $K = \frac{2\pi}{L}$ where L is the period of the stiffness modulation. Ω is a frequency associated with the velocity of the stiffness modulation, V . The quantities K and V are independent.

The sign of Ω determines the direction of propagation of the modulation. In this representation, the maximum stiffness of the material is $C_{11}^{\max} = C_0 + 2C_1$. If $C(x, t)$ were independent of position, then equation (41) would be symmetric in position and time, however as $C(x, t)$ depends on position, there is a term on the right side of equation (41) that is linear in position. This informs our choice of Bloch wave solutions in the spatial coordinate.

The periodicity of the modulated 1D medium suggests that we should be seeking solutions of equation (41) in the form of Bloch waves:

$$u(x, t) = \sum_k \sum_g u(k, g, t) e^{i(k+g)x}, \quad (43)$$

where $x \in [0, L]$. The wave number k is limited to the first Brillouin zone: $\left[-\frac{\pi}{L}, \frac{\pi}{L}\right]$ and $g = \frac{2\pi}{L}m$ with m being a positive or negative integer. With this choice of solution and inserting equation (43) into (41), the propagation of longitudinal waves is now described by:

$$\frac{\partial^2 u(k+g, t)}{\partial t^2} + v_a^2(k+g)^2 u(k+g, t) = i\varepsilon \{f(k')u(k', t)e^{i\Omega t} + h(k'')u(k'', t)e^{-i\Omega t}\}, \quad (44)$$

where $f(k) = Kk + k^2$, $h(k) = Kk - k^2$, $k' = k + g - K$ and $k'' = k + g + K$. In this equation, we have defined: $v_a^2 = \frac{C_0}{\rho}$ and $\varepsilon = \frac{C_1}{\rho}$. This equation is solved by using the multiple time scale perturbation method [36]. For the sake of analytical simplicity, ε is treated as a perturbation and we write the displacement as a second-order power series in the perturbation, namely:

$$u(k+g, \tau_0, \tau_1, \tau_2) = u_0(k+g, \tau_0, \tau_1, \tau_2) + \varepsilon u_1(k+g, \tau_0, \tau_1, \tau_2) + \varepsilon^2 u_2(k+g, \tau_0, \tau_1, \tau_2). \quad (45)$$

In equation (45), u_i with $i = 0, 1, 2$ are displacement functions expressed to zeroth-order, first-order and second-order in the perturbation. The single time variable, t , is also replaced by three variables representing different time scales: $\tau_0 = t$, $\tau_1 = \varepsilon t$, and $\tau_2 = \varepsilon^2 t = \varepsilon^2 \tau_0$. We can subsequently decompose equation (44) into three equations: one equation to zeroth-order in ε , one equation to first-order in ε and a third equation to second-order in ε . The zeroth-order equation represents the propagation of an elastic wave in a homogeneous medium.

$$\frac{\partial^2 u_0(k+g, \tau_0, \tau_1, \tau_2)}{\partial \tau_0^2} + v_a^2(k+g)^2 u_0(k+g, \tau_0, \tau_1, \tau_2) = 0. \quad (46)$$

Its solution is taking the form of the Bloch wave:

$$u_0(k+g, \tau_0, \tau_1, \tau_2) = a_0(k+g, \tau_1, \tau_2) e^{i\omega_0(k+g)\tau_0} \quad (47)$$

with the usual form: $\omega_0(k+g) = v_a|k+g|$.

The first-order equation is used to solve for u_1 .

$$\begin{aligned} & \frac{\partial^2 u_1(k+g, \tau_0, \tau_1, \tau_2)}{\partial \tau_0^2} + \omega_0^2(k+g) u_1(k+g, \tau_0, \tau_1, \tau_2) + 2 \frac{\partial^2 u_0(k+g, \tau_0, \tau_1, \tau_2)}{\partial \tau_1 \partial \tau_0} \\ & = i \{f(k')u_0(k', \tau_0, \tau_1, \tau_2)e^{i\Omega\tau_0} + h(k'')u_0(k'', \tau_0, \tau_1, \tau_2)e^{-i\Omega\tau_0}\}. \end{aligned} \quad (48)$$

The third term in equation (48) leads to secular terms and is set to zero by assuming that the displacement, $u_0(k+g, \tau_0, \tau_2)$ is not a function of τ_1 . The displacement at all orders of expansion is subsequently taken to be independent of odd time scales. The solution to equation (48) is obtained in the form of the sum of homogeneous and particular solutions:

$$\begin{aligned} u_1(k+g, \tau_0, \tau_2) &= a_1(k+g, \tau_2) e^{i\omega_0(k+g)\tau_0} + i \frac{f(k')a_0(k', \tau_2)}{\omega_0^2(k+g) - (\omega_0(k') + \Omega)^2 + i\varphi} e^{i(\omega_0(k') + \Omega)\tau_0} \\ &+ i \frac{h(k'')a_0(k'', \tau_2)}{\omega_0^2(k+g) - (\omega_0(k'') - \Omega)^2 + i\varphi} e^{i(\omega_0(k'') - \Omega)\tau_0}. \end{aligned} \quad (49)$$

A small damping term $i\varphi$ is introduced to address the divergence of the two resonances that occur at $\omega_0^2(k+g) = (\omega_0(k') + \Omega)^2$ and $\omega_0^2(k+g) = (\omega_0(k'') - \Omega)^2$. We will later take the limit $\varphi \rightarrow 0$. The particular solutions introduce additional dispersion curves in the band structure of the time-dependent superlattice obtained by shifting the zeroth-order band structure by $\pm\Omega$. This can be interpreted as the spatio-temporal modulation resulting in frequency splitting of a monochromatic incident signal that is analogous to Brillouin scattering [7].

Finally, the second-order equation of motion is given by:

$$\begin{aligned} \frac{\partial^2 u_2(k+g, \tau_0, \tau_2)}{\partial \tau_0^2} + \omega_0^2(k+g) u_2(k+g, \tau_0, \tau_2) + 2 \frac{\partial^2 u_0(k+g, \tau_0, \tau_2)}{\partial \tau_2 \partial \tau_0} \\ = i \{ f(k') u_1(k', \tau_0, \tau_2) e^{i\Omega \tau_0} + h(k'') u_1(k'', \tau_0, \tau_2) e^{-i\Omega \tau_0} \}. \end{aligned} \quad (50)$$

Inserting equation (49) into (50), leads to terms of the form $e^{i\omega_0(k+g)\tau_0}$ in the right-hand-side of the equation. These terms lead to secular behavior that can be canceled by equating them to the third term in the left-hand-side of the equation. One obtains

$$2 \frac{\partial^2 u_0(k+g, \tau_0, \tau_2)}{\partial \tau_2 \partial \tau_0} = -M(k+g, \Omega, K) a_0(k+g, \tau_2) e^{i\omega_0(k+g)\tau_0} \quad (51)$$

with

$$\begin{aligned} M(k+g, \Omega, K) = & \left\{ f(k') h(k+g) \left(\frac{1}{\omega_0^2(k') - (\omega_0(k+g) - \Omega)^2} \right) \right. \\ & \left. + h(k'') f(k+g) \left(\frac{1}{\omega_0^2(k'') - (\omega_0(k+g) + \Omega)^2} \right) \right\}. \end{aligned} \quad (52)$$

Introducing an amplitude of the form, $a_0(k+g, \tau_2) = \alpha_0(k+g) e^{i\gamma \tau_2}$, one may rewrite $u_0(k+g, \tau_0, \tau_2)$ as

$$u_0(k+g, \tau_0, \tau_2) = \alpha_0(k+g) e^{i\gamma \tau_2} e^{i\omega_0(k+g)\tau_0} = \alpha_0(k+g) e^{i[\omega_0(k+g) + \gamma \varepsilon^2] \tau_0} = \alpha_0(k+g) e^{i\omega_0^*(k+g)\tau_0}.$$

Then one obtains a correction to $\omega_0(k+g)$, leading to a frequency shift. This frequency shift is most pronounced for values of the wave number leading to strong resonances and is given by:

$$\delta\omega_0(k+g) = \omega_0^*(k+g) - \omega_0(k+g) = \varepsilon^2(\gamma)_{pp} = \frac{\varepsilon^2}{2\omega_0(k+g)} M(k+g, \Omega, K)_{pp}. \quad (53)$$

The symbol $(\square)_{pp}$ in this expression represents Cauchy's principle part that results from taking the limit: $\varphi \rightarrow 0$. This frequency shift is the signature of the formation of hybridization band gaps between the zeroth-order dispersion relation and first-order Brillouin scattered modes. The denominators of the resonance conditions: $\omega_0^2(k') - (\omega_0(k+g) - \Omega)^2 = 0$ and $\omega_0^2(k'') - (\omega_0(k+g) + \Omega)^2 = 0$ determine the location of the formation of the hybridization gaps. These conditions predict hybridization gaps where the lowest first-order dispersion branch ($g = 0$) and second lowest branch ($g = \frac{2\pi}{L}$) intersect a first-order Brillouin scattered dispersion curve. The two gaps form only on one side (positive or negative side) of the first Brillouin zone depending on the sign of Ω (i.e., the direction of propagation of the modulation of the stiffness). These two gaps occur at the same wave number: k_g . This leads to a band structure that does not possess mirror symmetry about the frequency axis. The band structure now possesses a center of inversion, the origin, rather than a mirror plane. When $M(k+g, \Omega, K) > 0$, one has $k > k_g$ and when $M(k+g, \Omega, K) < 0$, one has $k < k_g$.

We illustrate this effect schematically in figure 4.

3.2. Temporal phonon dirac equation and temporal ghost phonons

Our starting point is equation (51) which combined with equation (47) yields:

$$\frac{\partial^2 u_0(k+g, \tau_0, \tau_2)}{\partial \tau_2 \partial \tau_0} = -\frac{1}{2} M(k+g, \Omega, K) u_0(k+g, \tau_0, \tau_2). \quad (54)$$

It is also important to note that equation (51) is not a stand-alone equation but it is complemented by the zeroth-order equation of propagation (equation (46)).

We now introduce two new temporal variables, W and V such that:

$$\begin{cases} \tau_0 = W - V \\ \tau_2 = W + V. \end{cases} \quad (55)$$

These new variables can be expressed as:

$$\begin{cases} W = \frac{1}{2}(\tau_0 + \tau_2) = \frac{1}{2}(1 + \varepsilon^2)t \\ V = \frac{1}{2}(-\tau_0 + \tau_2) = -\frac{1}{2}(1 - \varepsilon^2)t \end{cases} \quad (56)$$

and represent a dilated time and the negative of a compressed time respectively.

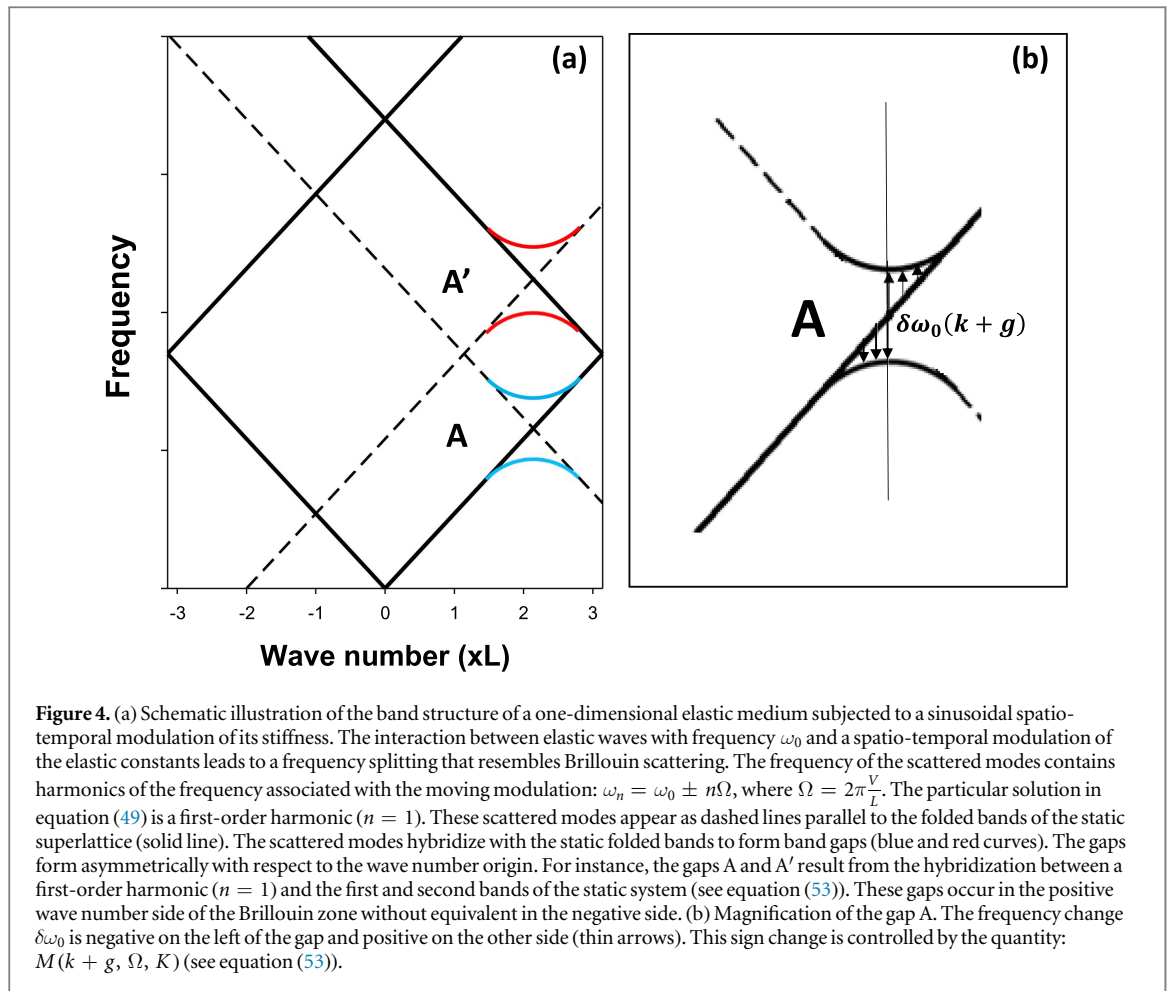


Figure 4. (a) Schematic illustration of the band structure of a one-dimensional elastic medium subjected to a sinusoidal spatio-temporal modulation of its stiffness. The interaction between elastic waves with frequency ω_0 and a spatio-temporal modulation of the elastic constants leads to a frequency splitting that resembles Brillouin scattering. The frequency of the scattered modes contains harmonics of the frequency associated with the moving modulation: $\omega_n = \omega_0 \pm n\Omega$, where $\Omega = 2\pi\frac{V}{L}$. The particular solution in equation (49) is a first-order harmonic ($n = 1$). These scattered modes appear as dashed lines parallel to the folded bands of the static superlattice (solid line). The scattered modes hybridize with the static folded bands to form band gaps (blue and red curves). The gaps form asymmetrically with respect to the wave number origin. For instance, the gaps A and A' result from the hybridization between a first-order harmonic ($n = 1$) and the first and second bands of the static system (see equation (53)). These gaps occur in the positive wave number side of the Brillouin zone without equivalent in the negative side. (b) Magnification of the gap A. The frequency change $\delta\omega_0$ is negative on the left of the gap and positive on the other side (thin arrows). This sign change is controlled by the quantity: $M(k + g, \Omega, K)$ (see equation (53)).

With this change in variables, equation (54) takes the form:

$$\frac{\partial^2 u_0(k + g, W, V)}{\partial W^2} - \frac{\partial^2 u_0(k + g, W, V)}{\partial V^2} + 2M(k + g, \Omega, K)u_0(k + g, W, V) = 0. \quad (57)$$

Equation (57) is the usual relativistic Klein–Gordon equation when $M(k + g, \Omega, K)$ is positive with the two temporal variables W and V playing the roles of ‘temporal’ and ‘spatial’ variables in the conventional; Klein–Gordon equation. $\sqrt{2M}$ is playing the role of ‘mass’. In the case of $M(k + g, \Omega, K) < 0$, then equation (57) is Klein–Gordon equation with an imaginary ‘mass’ $i\sqrt{2|M|}$.

3.3. Temporal Dirac phonons

This subsection addresses the behavior of the time-dependent superlattice when $M(k + g, \Omega, K) > 0$. In this case, following Dirac [32], equation (57) can be factored

$$\left[\sigma_x \frac{\partial}{\partial W} - i\sigma_y \frac{\partial}{\partial V} - i\alpha I \right] \psi = 0, \quad (58a)$$

$$\left[\sigma_x \frac{\partial}{\partial W} - i\sigma_y \frac{\partial}{\partial V} + i\alpha I \right] \bar{\psi} = 0, \quad (58b)$$

where again σ_x and σ_y are the 2×2 Pauli matrices: $\begin{pmatrix} 0 & 1 \\ 1 & 0 \end{pmatrix}$ and $\begin{pmatrix} 0 & -i \\ i & 0 \end{pmatrix}$ and I is the 2×2 identity matrix. We have renamed $\alpha = \sqrt{2M}$. These equations are isomorphic to equation (8).

We note that taking the complex conjugate of equation (58a) results in equation (58b), indeed the first two terms are real and only the last term changes sign. In particular, this results from the negative sign of the second term in the Klein–Gordon equation (57) which requires the multiplicative imaginary number ‘i’ on the second term of the Dirac equations. Then $\bar{\psi} = \psi^*$. So while ψ is a solution of equation (58a), its complex conjugate is not a solution of (58a). $\bar{\psi}$ is solution of equation (58b). In the language of quantum field theory, ψ and $\bar{\psi}$ represent the two different physical entities, namely ‘particles’ and ‘antiparticles.’

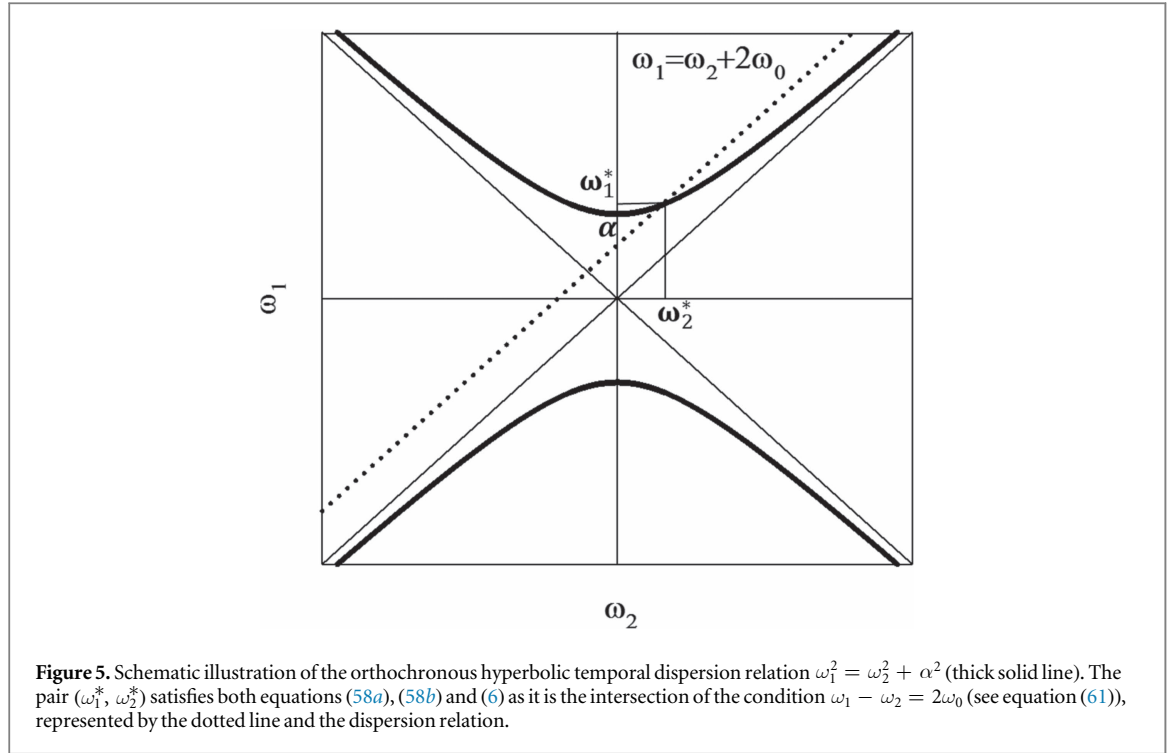


Figure 5. Schematic illustration of the orthochronous hyperbolic temporal dispersion relation $\omega_1^2 = \omega_2^2 + \alpha^2$ (thick solid line). The pair (ω_1^*, ω_2^*) satisfies both equations (58a), (58b) and (6) as it is the intersection of the condition $\omega_1 - \omega_2 = 2\omega_0$ (see equation (61)), represented by the dotted line and the dispersion relation.

We write our solutions in the form: $\psi(\omega_1, \omega_2) = \xi(\omega_1, \omega_2)e^{(\pm)i\omega_1 W}e^{(\pm)i\omega_2 V}$ and $\bar{\psi}(\omega_1, \omega_2) = \bar{\xi}(\omega_1, \omega_2)e^{(\pm)i\omega_1 W}e^{(\pm)i\omega_2 V}$ where $\xi = \begin{pmatrix} a_1 \\ a_2 \end{pmatrix}$ and $\bar{\xi} = \begin{pmatrix} \bar{a}_1 \\ \bar{a}_2 \end{pmatrix}$ are two by one spinors. Inserting the various forms for these solutions in equations ((58a), (58b)) lead to the ‘dispersion’ relation:

$$\omega_1^2 = \omega_2^2 + \alpha^2. \tag{59}$$

This is the equation of an orthochronous hyperbola in the (ω_1, ω_2) plane as illustrated in figure 5. However, as we have stated earlier, the pair (ω_1, ω_2) needs to also be compatible with the zeroth-order equation (46). For this, we write:

$$\omega_1 W + \omega_2 V = \tau_0 \left(\frac{\omega_1 - \omega_2}{2} \right) + \tau_2 \left(\frac{\omega_1 + \omega_2}{2} \right). \tag{60}$$

Since $u_0(k + g, \tau_0, \tau_2) = a_0(k + g, \tau_2)e^{i\omega_0(k+g)\tau_0}$, the pairs of frequencies (ω_1, ω_2) need to satisfy the condition:

$$\omega_1 - \omega_2 = 2\omega_0. \tag{61}$$

Inserting the condition given by equation (61) into (59) yields the additional condition:

$$\omega_1 + \omega_2 = \frac{M}{\omega_0}. \tag{62}$$

The graphical construction of the solutions of equations (58a), (58b) and (46) is given in figure 5. The solutions (ω_1^*, ω_2^*) evolve with the wave number k , as both ω_0 and α vary with k . By varying k over the interval $[-\frac{\pi}{L}, -k_g] - [k_g, \frac{\pi}{L}]$, and following the branch of the dispersion relation that possesses non-zero positive $M(k)$, $\omega_0(k)$ spans positive and negative values in the interval $[\omega_0(-\frac{\pi}{L}k_g), \omega_0(-k_g)] - [\omega_0(k_g), \omega_0(\frac{\pi}{L})]$.

Spanning this range enables us to explore the different positive and negative values of ω_1^* and ω_2^* , i.e., both top and bottom branches in figure 5. The spinor parts ξ and $\bar{\xi}$ for the different ‘orbital’ parts, $e^{(\pm)i\omega_1 W}e^{(\pm)i\omega_2 V}$ are collected in table 1 below.

Since both $\omega_1 - \omega_2$ and $\omega_1 + \omega_2$ are real positive quantities, the spinors in table 1 are real. Let us consider, as an example, the first entry in table 1 (i.e., the orbital part is $e^{+i\omega_1 W}e^{+i\omega_2 V}$), the spinor: $\xi = \begin{pmatrix} \sqrt{\omega_1 - \omega_2} \\ -\sqrt{\omega_1 + \omega_2} \end{pmatrix}$.

Inserting equations (61) and (62) yields $\xi_A = \begin{pmatrix} \sqrt{2\omega_0} \\ -\sqrt{\frac{M}{\omega_0}} \end{pmatrix}$. Considering the orbital part $e^{+i\omega_1 W}e^{-i\omega_2 V}$, the spinor

Table 1. Two by one spinor solutions of equations (58a) and (58b) for the different ‘orbital’ forms.

	$e^{+i\omega_1 W} e^{+i\omega_2 V}$	$e^{-i\omega_1 W} e^{+i\omega_2 V}$	$e^{+i\omega_1 W} e^{-i\omega_2 V}$	$e^{-i\omega_1 W} e^{-i\omega_2 V}$
ξ	$\begin{pmatrix} \sqrt{\omega_1 - \omega_2} \\ -\sqrt{\omega_1 + \omega_2} \end{pmatrix}$	$\begin{pmatrix} \sqrt{\omega_1 + \omega_2} \\ \sqrt{\omega_1 - \omega_2} \end{pmatrix}$	$\begin{pmatrix} \sqrt{\omega_1 + \omega_2} \\ -\sqrt{\omega_1 - \omega_2} \end{pmatrix}$	$\begin{pmatrix} \sqrt{\omega_1 - \omega_2} \\ \sqrt{\omega_1 + \omega_2} \end{pmatrix}$
$\bar{\xi}$	$\begin{pmatrix} \sqrt{\omega_1 - \omega_2} \\ \sqrt{\omega_1 + \omega_2} \end{pmatrix}$	$\begin{pmatrix} -\sqrt{\omega_1 + \omega_2} \\ \sqrt{\omega_1 - \omega_2} \end{pmatrix}$	$\begin{pmatrix} \sqrt{\omega_1 + \omega_2} \\ \sqrt{\omega_1 - \omega_2} \end{pmatrix}$	$\begin{pmatrix} -\sqrt{\omega_1 - \omega_2} \\ \sqrt{\omega_1 + \omega_2} \end{pmatrix}$

component becomes $\xi_B = \begin{pmatrix} \sqrt{\frac{M}{\omega_0}} \\ -\sqrt{2\omega_0} \end{pmatrix}$. In the limit of a small perturbation, $M(k) \rightarrow 0$ and

$$\xi_A = \begin{pmatrix} a_1 \\ 0 \end{pmatrix} = \begin{pmatrix} \sqrt{2\omega_0} \\ 0 \end{pmatrix} \text{ and } \xi_B = \begin{pmatrix} 0 \\ a_2 \end{pmatrix} = \begin{pmatrix} 0 \\ -\sqrt{2\omega_0} \end{pmatrix}. A \text{ and } B \text{ correspond to points along the right and left}$$

asymptotes of the top curve in figure 5. Under these conditions the orbital parts of A and B reduce to $e^{+i\omega_0\tau_0}$ and $e^{+i\frac{M}{\omega_0}\tau_2}$. Point A corresponds to an unperturbed solution of the wave equation i.e., solution in a homogeneous medium without modulation. Point B represents the effect of the perturbation. The components of a general spinor $\xi = \begin{pmatrix} a_1 \\ a_2 \end{pmatrix}$ measure the ‘amount’ of correction relative to the unmodulated solution in the space of the two time scales τ_0 and τ_2 .

Relations (61) and (62) enable us to express the spinors in terms of the wave number k . The parameter k (and simultaneously, $\omega_0(k)$), leads to measurable and subsequently tunable spinors ξ and $\bar{\xi}$.

We now define the quantity $s = \frac{\partial\omega_1}{\partial\omega_2}$. Using equation (59), we can obtain the following expression for the two frequencies ω_1 and ω_2 :

$$\omega_1 = \alpha\sqrt{1 + \gamma^2 s^2} = \alpha\gamma \quad (63a)$$

$$\omega_2 = \alpha\gamma s, \quad (63b)$$

where $\gamma = \frac{1}{\sqrt{1-s^2}}$. As noticeable in figure 5, for every solution (ω_1^*, ω_2^*) the quantity s is always less than 1 and γ is isomorphic to a Lorentz factor. Therefore, the temporal Dirac phonons described here behave like particles for which the quantity s must be less than 1.

3.4. Temporal ghost phonons

When $M(k + g, \Omega, K) < 0$. Equations (58a), (58b) become

$$\left[\sigma_x \frac{\partial}{\partial W} - i\sigma_y \frac{\partial}{\partial V} + \alpha' I \right] \psi_G = 0 \quad (64a)$$

$$\left[\sigma_x \frac{\partial}{\partial W} - i\sigma_y \frac{\partial}{\partial V} - \alpha' I \right] \bar{\psi}_G = 0, \quad (64b)$$

where $\alpha' = \sqrt{2|M|}$. These correspond to Dirac equations with an imaginary ‘mass’ $\alpha = i\alpha'$. These equations describe temporal ghost phonons also referred to as tachyons [30]. Seeking solutions in the form: $\psi_G(\omega_1, \omega_2) = \xi_G(\omega_1, \omega_2) e^{(\pm)i\omega_1 W} e^{(\pm)i\omega_2 V}$ and $\bar{\psi}_G(\omega_1, \omega_2) = c_0 \bar{\xi}_G(\omega_1, \omega_2) e^{(\pm)i\omega_1 W} e^{(\pm)i\omega_2 V}$ where ξ_G and $\bar{\xi}_G$ are also two by one spinors. Inserting the various forms for these solutions in equations (64a), (64b) lead to the ‘dispersion’ relation:

$$\omega_1^2 = \omega_2^2 - \alpha'^2. \quad (65)$$

This is the equation of an anti-chronous hyperbola in the (ω_1, ω_2) plane. Figure 6 shows this dispersion relation as well as the condition (61) that makes temporal ghost phonon solutions that are compatible with the zeroth-order equation (46).

Inserting equation (61) into (65) produces the condition:

$$\omega_1 + \omega_2 = -\frac{|M|}{\omega_0}. \quad (66)$$

Again, the solutions (ω_1^*, ω_2^*) for temporal ghost phonons evolve with the wave number, k , as both ω_0 and α vary with k . The temporal ghost phonons can be investigated by varying k over the intervals $[-k_g, k_g]$ and following the branch of the dispersion relation that possesses non-zero negative $M(k)$. Spanning this range enables us to explore the different positive and negative values of ω_1^* and ω_2^* , i.e., both left and right branches in figure 6. The spinor parts ξ_G and $\bar{\xi}_G$ for the different ‘orbital’ parts, $e^{(\pm)i\omega_1 W} e^{(\pm)i\omega_2 V}$ are collected in table 2 below.

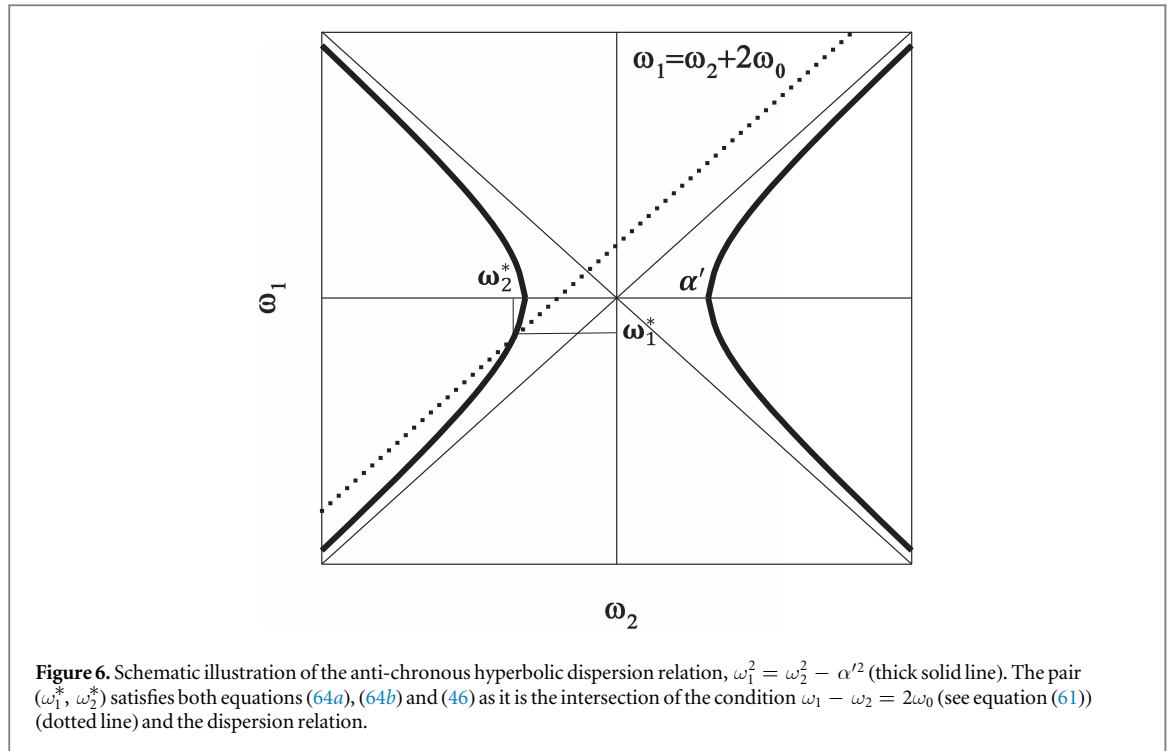


Table 2. Two by one spinor solutions of equations (64a), (64b) for the different ‘orbital’ forms.

	$e^{+i\omega_1 W} e^{+i\omega_2 V}$	$e^{-i\omega_1 W} e^{+i\omega_2 V}$	$e^{+i\omega_1 W} e^{-i\omega_2 V}$	$e^{-i\omega_1 W} e^{-i\omega_2 V}$
ξ_G	$\begin{pmatrix} i\sqrt{\omega_2 - \omega_1} \\ \sqrt{\omega_2 + \omega_1} \end{pmatrix}$	$\begin{pmatrix} i\sqrt{\omega_2 + \omega_1} \\ \sqrt{\omega_2 - \omega_1} \end{pmatrix}$	$\begin{pmatrix} i\sqrt{\omega_2 + \omega_1} \\ -\sqrt{\omega_2 - \omega_1} \end{pmatrix}$	$\begin{pmatrix} i\sqrt{\omega_2 - \omega_1} \\ -\sqrt{\omega_2 + \omega_1} \end{pmatrix}$
$\bar{\xi}_G$	$\begin{pmatrix} i\sqrt{\omega_2 - \omega_1} \\ -\sqrt{\omega_2 + \omega_1} \end{pmatrix}$	$\begin{pmatrix} -i\sqrt{\omega_2 + \omega_1} \\ \sqrt{\omega_2 - \omega_1} \end{pmatrix}$	$\begin{pmatrix} i\sqrt{\omega_2 + \omega_1} \\ \sqrt{\omega_2 - \omega_1} \end{pmatrix}$	$\begin{pmatrix} i\sqrt{\omega_2 - \omega_1} \\ \sqrt{\omega_2 + \omega_1} \end{pmatrix}$

Inserting equations (61) and (66) into the first entry of table 2, for example: $\xi_G = \begin{pmatrix} i\sqrt{\omega_2 - \omega_1} \\ \sqrt{\omega_2 + \omega_1} \end{pmatrix}$ yields

$\xi_G = i \begin{pmatrix} \sqrt{2\omega_0} \\ -\sqrt{|M|} \\ \omega_0 \end{pmatrix}$. The spinors in table 2 are purely imaginary. They are $\frac{\pi}{2}$ out of phase compared to the spinors of table 1.

Relations (61) and (66) enable us to express the spinors in terms of the wave number k . The parameter k (and simultaneously, $\omega_0(k)$), leads to measurable and subsequently tunable spinors ξ_G and $\bar{\xi}_G$.

We again use the quantity $s = \frac{\partial\omega_1}{\partial\omega_2}$ to characterize the properties of the ghost phonons. Using equation (65), we can obtain the following expression for the two frequencies ω_1 and ω_2 :

$$\omega_1 = i\alpha' \sqrt{1 + \gamma^2 s^2} = i\alpha' \gamma \tag{67a}$$

$$\omega_2 = i\alpha' \gamma s, \tag{67b}$$

where again $\gamma = \frac{1}{\sqrt{1-s^2}}$. However, here, as seen in figure 6, s is always greater than 1 for every solution (ω_1^*, ω_2^*) .

The γ factor is subsequently an imaginary number $\gamma = \frac{i}{\sqrt{s^2-1}}$ which makes ω_1 and ω_2 real quantities. The ghost phonons described here behave like particles for which the quantity s is larger than 1. The lines $\omega_1 = \pm\omega_2$ in figures 5 and 6 serve as boundaries between temporal Dirac phonons and temporal ghost phonons i.e., particles with $s < 1$ and particles with $s > 1$. Equivalently, we can say that we can approach the band gap from one side or the other in momentum space without being able to cross the gap. The temporal ghost phonons are metaphors for superluminal particles while temporal Dirac phonons can be visualized as particles that do not exceed the ‘speed’ $s = 1$.

The temporal Dirac phonons and temporal ghost phonons discussed here obey a Dirac-like equation in a two-dimensional temporal space (compressed time and dilated time). These ‘particles’ possess Fermion

character i.e., obey a constraint reminiscent of Pauli's exclusion principle. That constraint relates to the interdependence of the components of the spinor $\begin{pmatrix} a_1 \\ a_2 \end{pmatrix}$. Following section 2, one can verify easily that spinors in tables 1 and 2 satisfy the spin $\frac{1}{2}$ eigenstate equation:

$$\left(\omega_2 \frac{\partial}{\partial \omega_1} + \omega_1 \frac{\partial}{\partial \omega_2} \right) \begin{pmatrix} a_1 \\ a_2 \end{pmatrix} = \frac{1}{2} \begin{pmatrix} a_1 \\ a_2 \end{pmatrix}.$$

3.5. Metrics and geodesics

In this section, we illustrate some additional properties of temporal Dirac phonons and temporal ghost phonons. In particular, we address their description in the context of a multi-dimensional curved temporal space.

3.5.1. Temporal metrics

In the case of a dynamical system that obeys a general second-order hyperbolic partial differential equation that supports wave excitations:

$$F(x_\mu, \phi, \partial_\mu \phi, \partial_\nu \partial_\mu \phi) = 0. \quad (68)$$

It is possible to obtain a geometrical description by defining an effective metric [37].

Linearizing equation (68) around some solution:

$$\phi(x_\mu, t) = \phi_0(x_\mu, t) + \varepsilon \phi_1(x_\mu, t) + \dots \quad (69)$$

yields

$$\frac{\partial F}{\partial(\partial_\mu \partial_\nu \phi)} \Big|_0 \partial_\mu \partial_\nu \phi_1 + \frac{\partial F}{\partial(\partial_\mu \phi)} \Big|_0 \partial_\mu \phi_1 + \frac{\partial F}{\partial(\phi)} \Big|_0 \phi_1 = 0. \quad (70)$$

Equation (69) can be rewritten as:

$$\partial_\mu \left\{ \frac{\partial F}{\partial(\partial_\mu \partial_\nu \phi)} \Big|_0 \partial_\nu \phi_1 \right\} + \left\{ \frac{\partial F}{\partial(\partial_\mu \phi)} \Big|_0 - \partial_\mu \left(\frac{\partial F}{\partial(\partial_\mu \partial_\nu \phi)} \Big|_0 \right) \right\} \partial_\mu \phi_1 + \frac{\partial F}{\partial(\phi)} \Big|_0 \phi_1 = 0. \quad (71)$$

It is therefore possible to define the contravariant metric tensor

$$f^{\mu\nu} = \sqrt{|g|} g^{\mu\nu} = \frac{\partial F}{\partial(\partial_\mu \partial_\nu \phi)} \Big|_0. \quad (72)$$

The second and third terms in equation (71) may be viewed as forming the analog of a vector potential and a scalar potential, respectively.

We can now reconstruct the perturbative series of the wave equation of the modulated system in terms of solution corrected to second-order. For this, we multiply equation (54) by ε^2 and combine it with equation (46). We also rename u_0 by u'_0 to reflect the corrected nature of the solution i.e., this is the solution that satisfies both the zeroth-order equation (46) and (54) which imposes corrections due to second-order effects. The wave equation including second-order corrections becomes:

$$\frac{\partial^2 u'_0(k+g, \tau_0, \tau_2)}{\partial \tau_0^2} + 2\varepsilon^2 \frac{\partial^2 u'_0(k+g, \tau_0, \tau_2)}{\partial \tau_2 \partial \tau_0} + \{v_a^2(k+g)^2 + \varepsilon^2 M(k+g, \Omega, K)\} u'_0(k+g, \tau_0, \tau_2) = 0. \quad (73)$$

For reasons that will be apparent in the upcoming derivations, we divide throughout equation (73) by $\frac{1}{\varepsilon^2}$ and obtain:

$$\frac{1}{\varepsilon^2} \frac{\partial^2 u'_0(k+g, \tau_0, \tau_2)}{\partial \tau_0^2} + \frac{\partial^2 u'_0(k+g, \tau_0, \tau_2)}{\partial \tau_2 \partial \tau_0} + \frac{\partial^2 u'_0(k+g, \tau_0, \tau_2)}{\partial \tau_0 \partial \tau_2} + \left\{ \frac{1}{\varepsilon^2} v_a^2(k+g)^2 + M(k+g, \Omega, K) \right\} u'_0(k+g, \tau_0, \tau_2) = 0. \quad (74)$$

Expanding equation (74) around a phonon vacuum i.e., no elastic displacement, then u'_0 plays the role of ϕ_1 . We can then define the contravariant metric tensor using relation (72).

We find:

$$[f^{\mu\nu}] = \begin{pmatrix} 1 & 1 \\ \varepsilon^2 & 0 \\ 1 & 0 \end{pmatrix}. \quad (75)$$

The determinant of that matrix is -1 , so we can define the contravariant metric tensor:

$$[g^{\mu\nu}] = \begin{pmatrix} 1 & 1 \\ \varepsilon^2 & 0 \\ 1 & 0 \end{pmatrix}. \quad (76)$$

We take the inverse of $[g^{\mu\nu}]$ to obtain the covariant metric tensor:

$$[g_{\mu\nu}] = \begin{pmatrix} 0 & -1 \\ -1 & \frac{1}{\varepsilon^2} \end{pmatrix}. \quad (77)$$

The temporal line element in the (τ_0, τ_2) space is then calculated as:

$$ds^2 = (d\tau_2, d\tau_0) \begin{pmatrix} 0 & -1 \\ -1 & \frac{1}{\varepsilon^2} \end{pmatrix} \begin{pmatrix} d\tau_2 \\ d\tau_0 \end{pmatrix} = \frac{1}{\varepsilon^2} d\tau_0^2 - 2d\tau_0 d\tau_2. \quad (78)$$

The off-diagonal terms in the metric tensor lead to a line element that is characteristic of a non-Euclidian (τ_0, τ_2) space.

If we focus on the part of the line element (equation (77)) that arises from the off-diagonal terms of equation (78), namely $d\tau_0 d\tau_2$, we can express it in terms of the temporal variables W and V using equation (55):

$$d\tau_0 d\tau_2 = (dW - dV)(dW + dV) = dW^2 - dV^2.$$

This is a line element in a two-dimensional temporal Minkowski space with an analog to the speed of light taken as '1.'

3.5.2. Space-multiple times (1 + 2) geometrical model

We consider the purely geometrical interpretation of the propagation of elastic waves in the time-dependent superlattice. That is, we introduce the potential into the curvature of spacetime. We start with equation (73) which is reformulated as:

$$\frac{\partial^2 \psi(k + g, \tau_0, \tau_2)}{\partial \tau_0^2} + 2\varepsilon^2 \frac{\partial^2 \psi(k + g, \tau_0, \tau_2)}{\partial \tau_2 \partial \tau_0} + N(k + g, \varepsilon, \Omega, K) \psi(k + g, \tau_0, \tau_2) = 0, \quad (79a)$$

where $N(k + g, \varepsilon, \Omega, K) = \{v_a^2(k + g)^2 + \varepsilon^2 M(k + g, \Omega, K)\}$. It is worth noting that N is always a positive quantity. While $M(k + g, \Omega, K)$ is positive for the temporal Dirac phonons, it is negative for the temporal ghost phonons. In the latter case, if $(k + g)$ (or k_g) is not too close to the origin, the small coefficient ε^2 makes $\varepsilon^2 M(k + g, \Omega, K)$ small compared to $\omega_0^2 = v_a^2(k + g)^2$ enforcing $N > 0$.

In equation (78), we have replaced the symbol u'_0 by ψ for ease of notation. We want to derive equation (78) from purely geometrical arguments. In the three-dimensional spacetime (ψ, τ_0, τ_2) , we define the line element:

$$dl^2 = d\psi^2 - N\psi^2 \frac{1}{1 - \varepsilon^2} \left(d\tau_0^2 - \frac{1}{\varepsilon^2} d\tau_2^2 \right). \quad (79b)$$

We consider a curve between two fixed point A and B . The length along the curve is:

$$L = \int_A^B dl = \int_A^B \sqrt{\left(\frac{\partial \psi}{\partial \lambda} \right)^2 - N\psi^2 \frac{1}{1 - \varepsilon^2} \left(\left(\frac{\partial \tau_0}{\partial \lambda} \right)^2 - \frac{1}{\varepsilon^2} \left(\frac{\partial \tau_2}{\partial \lambda} \right)^2 \right)} d\lambda = \int_A^B F d\lambda. \quad (80)$$

In equation (80) the curve is described in terms of the parameter, λ . To find a minimum of the length, $\delta L = 0$, we utilize the Euler–Lagrange equation:

$$\frac{\partial}{\partial \lambda} \left(\frac{\partial F}{\partial \left(\frac{\partial \psi}{\partial \lambda} \right)} \right) + \frac{\partial}{\partial \lambda} \left(\frac{\partial F}{\partial \left(\frac{\partial \tau_0}{\partial \lambda} \right)} \right) + \frac{\partial}{\partial \lambda} \left(\frac{\partial F}{\partial \left(\frac{\partial \tau_2}{\partial \lambda} \right)} \right) - \frac{\partial F}{\partial \psi} - \frac{\partial F}{\partial \tau_0} - \frac{\partial F}{\partial \tau_2} = 0 \quad (81)$$

$$\begin{aligned} & \frac{\partial}{\partial \lambda} \left\{ 2 \frac{\partial \psi}{\partial \lambda} - 2N\psi^2 \frac{1}{1 - \varepsilon^2} \left(\frac{\partial \tau_0}{\partial \lambda} - \frac{1}{\varepsilon^2} \frac{\partial \tau_2}{\partial \lambda} \right) \right\} + 2N\psi \frac{1}{1 - \varepsilon^2} \left(\left(\frac{\partial \tau_0}{\partial \lambda} \right)^2 - \frac{1}{\varepsilon^2} \left(\frac{\partial \tau_2}{\partial \lambda} \right)^2 \right) \\ & - \frac{1}{2} \frac{1}{G} \frac{\partial G}{\partial \lambda} \left\{ 2 \frac{\partial \psi}{\partial \lambda} - 2N\psi^2 \frac{1}{1 - \varepsilon^2} \left(\frac{\partial \tau_0}{\partial \lambda} - \frac{1}{\varepsilon^2} \frac{\partial \tau_2}{\partial \lambda} \right) \right\} = 0. \end{aligned} \tag{82}$$

We have defined $G = F^2$. We now chose $d\lambda = dl$ such that $F = G = 1$ and $\frac{\partial G}{\partial \lambda} = 0$. Equation (82) reduces to the first two terms. Expanding the derivative, $\frac{\partial}{\partial \lambda}$, one gets:

$$\begin{aligned} & 2 \frac{\partial^2 \psi}{\partial l^2} - 2N2\psi \frac{\partial \psi}{\partial l} \frac{1}{1 - \varepsilon^2} \left(\frac{\partial \tau_0}{\partial l} - \frac{1}{\varepsilon^2} \frac{\partial \tau_2}{\partial l} \right) - 2N\psi^2 \frac{1}{1 - \varepsilon^2} \left(\frac{\partial^2 \tau_0}{\partial l^2} - \frac{1}{\varepsilon^2} \frac{\partial^2 \tau_2}{\partial l^2} \right) \\ & + 2N\psi \frac{1}{1 - \varepsilon^2} \left(\left(\frac{\partial \tau_0}{\partial l} \right)^2 - \frac{1}{\varepsilon^2} \left(\frac{\partial \tau_2}{\partial l} \right)^2 \right) = 0. \end{aligned} \tag{83}$$

This is the equation of a geodesic. Along the geodesic $dl = v dt$ with a constant v . Furthermore, we recall that $\tau_0 = t$ and $\tau_2 = \varepsilon^2 t$. Inserting these into equation (82) results in:

$$\frac{\partial^2 \psi}{\partial t^2} + N\psi = \frac{\partial^2 \psi}{\partial \tau_0^2} + 2\varepsilon^2 \frac{\partial^2 \psi}{\partial \tau_0 \partial \tau_2} + N\psi = 0. \tag{84}$$

Equation (84) is indeed (78). To obtain equation (84), we used the following:

$$\begin{aligned} \frac{\partial \tau_0}{\partial l} - \frac{1}{\varepsilon^2} \frac{\partial \tau_2}{\partial l} &= \frac{1}{v} \left(\frac{\partial \tau_0}{\partial t} - \frac{1}{\varepsilon^2} \frac{\partial \tau_2}{\partial t} \right) = \frac{1}{v} \left(1 - \frac{1}{\varepsilon^2} \varepsilon^2 \right) = 0 \\ \frac{\partial^2 \tau_0}{\partial t^2} &= \frac{\partial^2 \tau_2}{\partial t^2} = 0 \end{aligned}$$

and

$$\frac{1}{1 - \varepsilon^2} \left(\left(\frac{\partial \tau_0}{\partial t} \right)^2 - \frac{1}{\varepsilon^2} \left(\frac{\partial \tau_2}{\partial t} \right)^2 \right) = \frac{1}{1 - \varepsilon^2} \left(1 - \frac{1}{\varepsilon^2} \varepsilon^4 \right) = 1.$$

The later approximation maintains equation (84) to second-order in ε . We note that it is the introduction of two time scales τ_0, τ_2 which enables us to obtain equation (84) from $\delta L = 0$.

To second-order (see equation (53))

$$N(k + g, \varepsilon, \Omega, K) \sim (\omega_0^*(k + g))^2. \tag{85}$$

The line element given by equation (79a) can then be rewritten as:

$$dl^2 = d\psi^2 - \psi^2 (\omega_0^*(k + g))^2 \frac{1}{1 - \varepsilon^2} \left(d\tau_0^2 - \frac{1}{\varepsilon^2} d\tau_2^2 \right). \tag{86}$$

This line element defines the metric tensor in the three-dimensional space (ψ, τ_0, τ_2) ,

$$[g] = \begin{pmatrix} 1 & 0 & 0 \\ 0 & -\psi^2 (\omega_0^*(k + g))^2 \frac{1}{1 - \varepsilon^2} & 0 \\ 0 & 0 & \frac{1}{\varepsilon^2} \psi^2 (\omega_0^*(k + g))^2 \frac{1}{1 - \varepsilon^2} \end{pmatrix}. \tag{87}$$

Equation (86) is reminiscent of the usual line element in polar coordinates, (ρ, θ) :

$$ds^2 = d\rho^2 + \rho^2 d\theta^2$$

with the role of the radial variable, ρ , played by ψ (i.e., the amplitude of the elastic wave). The angular variable is related to the two temporal variables scales τ_0, τ_2 via:

$$d\theta^2 = -(\omega_0^*(k + g))^2 \frac{1}{1 - \varepsilon^2} \left(d\tau_0^2 - \frac{1}{\varepsilon^2} d\tau_2^2 \right). \tag{88}$$

This result is different from equation (77) as the line element of equation (86) includes the effect of the potential: $V(\psi) = \frac{1}{2} N(k + g, \varepsilon, \Omega, K) \psi^2$ in the geometrical description.

We also note that with $d\tau_0 = dt$ and $d\tau_2 = \varepsilon^2 dt$, the line element $d\theta^2 = -(\omega_0^*(k + g))^2 dt^2$ (i.e., $d\theta = i\omega_0^*(k + g) dt$). The line element (86) reduces to the line element in the complex plane in polar coordinates.

We can see this from another point of view. We can rewrite equation (88) as a non-Euclidian Minkowski-like metric with two time-related variables:

$$d\theta^2 = dX_0^2 - \frac{1}{\varepsilon^2} dX_2^2 \quad (89)$$

with $X_0 = i\omega_0^*(k + g) \frac{1}{\sqrt{1-\varepsilon^2}} \tau_0$ and $X_2 = i\omega_0^*(k + g) \frac{1}{\sqrt{1-\varepsilon^2}} \tau_2$. The space spanned by the variables X_0 and X_2 is conical:

$$X_0^2 - \frac{1}{\varepsilon^2} X_2^2 = 0 \quad (90)$$

which implies $\tau_2 = \pm \varepsilon^2 \tau_0$; the positive solution being the one that defined τ_2 .

Equation (86) becomes

$$dI^2 = d\psi^2 - \psi^2 d\theta^2. \quad (91)$$

Again, this is the polar coordinate representation in the complex plane of: $(\psi, i\theta)$. The temporal variation of ψ was found to be: $\psi = \alpha(k + g) e^{i\omega_0^*(k+g)t}$. This is a normal mode of the time-dependent superlattice with second-order correction to the frequency which follows a nonlinear trajectory in the (ψ, t) plane. One can describe these solutions with a geometric approach. For instance, we can obtain the wave equation (84) from a purely geometrical argument in the space of ψ by introducing the line element:

$$ds^2 = 2(E - V(\psi)) d\psi^2. \quad (92)$$

This wave equation is the equation of a geodesic in a 1D curved space, ψ , with the metric $g = \sqrt{2(E - V(\psi))}$.

The dynamics of the elastic medium subjected to a spatio-temporal modulation of its stiffness was shown to be describable with a complex metric tensor. Scalar fields corresponding to complex metric tensors are known to possess tachyonic solutions [38].

4. Conclusions

We have developed spacetime representations of elastic waves in intrinsic and extrinsic topological phononic systems. Time-reversal and parity symmetries are broken individually in an intrinsic topological phononic structure through internal resonances. This is accomplished by attaching every mass in a 1D harmonic chain to a rigid substrate via side springs. The dynamical equations then take the form of the Klein–Gordon equation which when Dirac factored reveals the spinor nature of the elastic waves. These Dirac phonons possess fermion-like topologies and can be described within the context of quantum field theory [2]. Dirac phonon states are analogous to the usual spin but with states projected on the directions of propagation of the elastic waves along the harmonic chain. Dirac phonons behave like pseudospins. We explore the solutions of the dynamical equations in the form of contour integrals which enables us to connect the field theoretical description of topological elastic waves, their spacetime representation and the twistor theory. We have also considered an extrinsic topological phononic system composed of a 1D elastic medium supporting a spatio-temporal modulation of its stiffness. Spatio-temporal modulations break both parity and time-reversal symmetry leading to spectral non-reciprocity and the formation of band gaps in the elastic band structure that are asymmetric with respect to momentum. In the context of multiple time scale perturbation theory, we demonstrate an analogy between the longitudinal phonons in the vicinity of an asymmetric gap and two types of particle excitations, namely temporal Dirac particles and temporal ghost particles. These particles are defined in a two-dimensional time space. The Dirac phonons have a real ‘mass’ and the ghost phonons possess an imaginary ‘mass.’ The wave function of both types of phonons has amplitude that takes the form of (2×1) spinors. The spinors of ghost phonons, however, are phase shifted by $\frac{\pi}{2}$ with respect to their Dirac counterparts. We show that these two types of temporal phonons live on two separate sides of ghost lines. The ghost lines are analogous to introducing a limiting ‘velocity’ such as the speed of light in conventional spacetime. We map the spinor characteristics of temporal Dirac and ghost phonons to the dispersion curves in the elastic band structure. The spinor of each type of phonon is therefore measurable and tunable. Finally, we develop a purely geometric description of temporal Dirac and ghost phonons in curved 2D time. We show that the dynamics of Dirac and ghost phonons can be represented in the form of a geodesic in a complex spacetime.

The analogies between topological phononic systems, quantum field theory and spacetime representations open new avenues for the simultaneous investigation of both scalar quantum field and general relativistic analogs in a single experiment. The twistor space representation of Dirac phonons but also temporal Dirac phonons with pseudospin characteristics presents opportunities to study the relationship between twistor theory and quantum field theories. The introduction of temporal ghost phonons also creates new approaches to

both the modeling and measurement of analog tachyonic behavior. It can be further noted that the investigation of these elastic analogs and their parameters is entirely at the choice of the experimenter. Hence, we see that the analogy between the elastic behavior of intrinsic and extrinsic topological phononic structures and the scalar quantum field theory and general relativity allows for the experimental exploration of a number of concepts and of exotic particle excitations that previously have only been theorized.

Authors' contributions

PAD and KR conceived the models and performed many of the analytical mathematical calculations, interpreted them and wrote the paper. PL contextualized the work. JOV performed some of the analytical calculations. All authors discussed the results and commented on the manuscript and gave final approval for publication.

Funding

This work was supported by National Science Foundation award EFRI # 1640860.

Data accessibility statement

This work does not have any data.

Competing interests statement

We have no competing interests.

ORCID iDs

Pierre A Deymier  <https://orcid.org/0000-0002-1088-7958>

References

- [1] Deymier P A (ed) 2013 *Acoustic Metamaterials and Phononic Crystals (Springer Series in Solid State Sciences vol 173)* (Berlin: Springer)
- [2] Deymier P A and Runge K 2017 *Sound Topology, Duality, Coherence and Wave-Mixing: An Introduction to the Emerging New Science of Sound (Springer Series in Solid State Sciences vol 188)* (Berlin: Springer)
- [3] Deymier P A, Runge K, Swintek N and Muralidharan K 2015 Torsional topology and fermion-like behavior of elastic waves in phononic structures *C. R. Acad. Bulg. Sci.* **343** 700–11
- [4] Deymier P A, Runge K, Swintek N and Muralidharan K 2014 Rotational modes in a phononic crystal with fermion-like behaviour *J. Appl. Phys.* **115** 163510
- [5] Swintek N, Matsuo S, Runge K, Vasseur J O, Lucas P and Deymier P A 2015 Bulk elastic waves with unidirectional backscattering-immune topological states in a time-dependent superlattice *J. Appl. Phys.* **118** 063103
- [6] Deymier P A, Gole V, Lucas P, Vasseur J O and Runge K 2017 Tailoring phonon band structures with broken symmetry by shaping spatiotemporal modulations of stiffness in a one-dimensional elastic waveguide *Phys. Rev. B* **96** 064304
- [7] Croënne C, Vasseur J O, Bou Matar O, Ponge M-F, Deymier P A, Hladky-Hennion A-C and Dubus B 2017 Brillouin scattering-like effect and non-reciprocal propagation of elastic waves due to spatio-temporal modulation of electrical boundary conditions in piezoelectric media *Appl. Phys. Lett.* **110** 061901
- [8] Trainiti G and Ruzzene M 2016 Non-reciprocal elastic wave propagation in spatio-temporal periodic structures *New J. Phys.* **18** 083047
- [9] Nassar H, Xu X, Norris A and Huang G 2017 Modulated phononic crystals: non-reciprocal wave propagation and Willis materials *J. Mech. Phys. Solids* **101** 10
- [10] Nassar H, Chen H, Norris A and Huang G 2017 Non-reciprocal flexural wave propagation in a modulated metabeam *Extreme Mech. Lett.* **15** 97
- [11] Deymier P A and Runge K 2016 One-dimensional mass-spring chains supporting elastic waves with non-conventional topology *Crystals* **6** 44
- [12] Huber S D 2016 Topological mechanics *Nat. Phys.* **12** 621 and references therein
- [13] Liu Y, Xu Y, Zhang S-C and Duan W 2017 Model for topological phononics and phonon diode *Phys. Rev. B* **96** 064106
- [14] Maxwell J C 1865 A dynamical theory of the electromagnetic field *Phil. Trans. R. Soc. A* **155** 459
- [15] Weaver R L 1990 Anderson localization of ultrasound *Wave Motion* **12** 129
- [16] Hu H F, Strybulevych A, Page J H, Skipetrov S E and Van Tiggelen B A 2008 Localization of ultrasound in a three-dimensional elastic network *Nat. Phys.* **4** 945
- [17] Van der Biest F, Sukhovich A, Tourin A, Page J H, van Tiggelen B A, Liu Z and Fink M 2005 Resonant tunneling of acoustic waves through a double barrier of two phononic crystals *Europhys. Lett.* **71** 63

- [18] Yang S, Page J H, Zhengyou L, Cowan M L, Chan C T and Sheng P 2002 Ultrasound tunneling through 3D phononic crystals *Phys. Rev. Lett.* **88** 104301
- [19] Unruh W G 1981 Experimental black-hole evaporation? *Phys. Rev. Lett.* **46** 1351
- [20] Fang K, Yu Z and Fan S 2012 Photonic Aharonov–Bohm effect based on dynamic modulation *Phys. Rev. Lett.* **108** 153901
- [21] Fang K, Yu Z and Fan S 2012 Realizing effective magnetic field for photons by controlling the phase of dynamic modulation *Nat. Photon.* **6** 782
- [22] Tzuang L, Fang K, Nussenzeig P, Fan S and Lipson M 2014 Non-reciprocal phase shift induced by an effective magnetic flux for light *Nat. Photon.* **8** 701
- [23] Li E, Eggleton B J, Fang K and Fan S 2014 Photonic aharonov-bohm effect in photon–photon interactions *Nat. Commun.* **5** 3225
- [24] Aharonov Y, Komar A and Susskind L 1969 Superluminal behavior, causality and instability *Phys. Rev.* **182** 1400
- [25] Woodhouse N M J 1992 Contour integrals for the ultrahyperbolic wave equation *Proc. R. Soc. A* **438** 197
- [26] Penrose R 1967 Twistor algebra *J. Math. Phys.* **8** 345
- [27] Silveirinha M G 2015 Chern invariants for continuous media *Phys. Rev. B* **92** 125153
- [28] Silveirinha M G 2016 Z_2 topological index for continuous photonic materials *Phys. Rev. B* **93** 075110
- [29] Berry M V 1984 Quantal phase factors accompanying adiabatic changes *Proc. R. Soc. A* **392** 45
- [30] Feinberg G 1967 Possibility of faster-than-light particles *Phys. Rev.* **159** 1089
- [31] Hodges A P 1985 Mass eigenstates in twistor theory *Proc. R. Soc. A* **397** 375
- [32] Dirac P A M 1928 The quantum theory of the electron *Proc. R. Soc. A* **117** 778
- [33] Elachi C 1972 Dipole antenna in space-time periodic media *IEEE Trans. Antennas Propag.* **20** 280
- [34] Hadad Y, Sounas D L and Alu A 2015 Space-time gradient metasurfaces *Phys. Rev. B* **92** 100304 (R)
- [35] Lira H, Yu Z, Fan S and Lipson M 2012 Electrically driven nonreciprocity induced by interband photonic transition on a silicon chip *Phys. Rev. Lett.* **109** 033901
- [36] Khoo I C and Wang Y K 1976 Multiple time scale analysis of an anharmonic crystal *J. Math. Phys.* **17** 222
- [37] Barcelo C, Liberati S and Visser M 2001 Analog gravity from field theory normal modes? *Class. Quantum Grav.* **18** 3595
- [38] Kao W F 2001 Induced gravity with complex metric field arXiv:[hep-th/0008124](https://arxiv.org/abs/hep-th/0008124)